

## Article

# Assessment of Groundwater Quality Using the Pollution Index of Groundwater (PIG), Nitrate Pollution Index (NPI), Water Quality Index (WQI), Multivariate Statistical Analysis (MSA), and GIS Approaches: A Case Study of the Mnasra Region, Gharb Plain, Morocco

Hatim Sanad <sup>1,2,\*</sup>, Latifa Mouhir <sup>1</sup>, Abdelmjid Zouahri <sup>2</sup>, Rachid Moussadek <sup>3</sup>, Hamza El Azhari <sup>4</sup>, Hasna Yachou <sup>2</sup>, Ahmed Ghanimi <sup>5</sup>, Majda Oueld Lhaj <sup>1,2</sup> and Houria Dakak <sup>2</sup>

- <sup>1</sup> Laboratory of Process Engineering and Environment, Faculty of Science and Technology Mohammedia, University Hassan II of Casablanca, Mohammedia 28806, Morocco; latifa.mouhir@fstm.ac.ma (L.M.); majdaoueldlhaj1999@gmail.com (M.O.L.)
  - <sup>2</sup> Research Unit on Environment and Conservation of Natural Resources, Regional Center of Rabat, National Institute of Agricultural Research, AV. Ennasr, Rabat 10101, Morocco; abdelmjid.zouahri@inra.ma (A.Z.); yachou@inra.ma (H.Y.); houria.dakak@inra.ma (H.D.)
  - <sup>3</sup> International Center for Agricultural Research in the Dry Areas (ICARDA), Rabat P.O. Box 2034, Morocco; r.moussadek@cgiar.org
  - <sup>4</sup> Laboratory of Physical Chemistry of Materials, Natural Substances and Environment, Chemistry Department, Sciences, and Technology Faculty, Abdelmalek Essaâdi University, Tangier 90090, Morocco; hamza.elazhari@etu.uae.ac.ma
  - <sup>5</sup> Laboratory of Materials, Nanotechnologies, and Environment, Department of Chemistry, Faculty of Sciences, Mohammed V University in Rabat, Rabat 10101, Morocco; ghanimiahmed@gmail.com
- \* Correspondence: hatim.sanad99@gmail.com



**Citation:** Sanad, H.; Mouhir, L.; Zouahri, A.; Moussadek, R.; El Azhari, H.; Yachou, H.; Ghanimi, A.; Oueld Lhaj, M.; Dakak, H. Assessment of Groundwater Quality Using the Pollution Index of Groundwater (PIG), Nitrate Pollution Index (NPI), Water Quality Index (WQI), Multivariate Statistical Analysis (MSA), and GIS Approaches: A Case Study of the Mnasra Region, Gharb Plain, Morocco. *Water* **2024**, *16*, 1263. <https://doi.org/10.3390/w16091263>

Academic Editors: Chi-Feng Chen and Chia-Ling Chang

Received: 31 March 2024

Revised: 12 April 2024

Accepted: 18 April 2024

Published: 28 April 2024



**Copyright:** © 2024 by the authors. Licensee MDPI, Basel, Switzerland. This article is an open access article distributed under the terms and conditions of the Creative Commons Attribution (CC BY) license (<https://creativecommons.org/licenses/by/4.0/>).

**Abstract:** Groundwater, an invaluable resource crucial for irrigation and drinking purposes, significantly impacts human health and societal advancement. This study aims to evaluate the groundwater quality in the Mnasra region of the Gharb Plain, employing a comprehensive analysis of thirty samples collected from various locations, based on thirty-three physicochemical parameters. Utilizing tools like the Pollution Index of Groundwater (PIG), Nitrate Pollution Index (NPI), Water Quality Index (WQI), Irrigation Water Quality Index (IWQI), as well as Multivariate Statistical Approaches (MSA), and the Geographic Information System (GIS), this research identifies the sources of groundwater pollution. The results revealed  $\text{Ca}^{2+}$  dominance among cations and  $\text{Cl}^-$  as the primary anion. The Piper and Gibbs diagrams illustrated the prevalent  $\text{Ca}^{2+}\text{-Cl}^-$  water type and the significance of water–rock interactions, respectively. The PIG values indicated that 86.66% of samples exhibited “Insignificant pollution”. NPI showed notable nitrate pollution (1.48 to 7.06), with 83.33% of samples rated “Good” for drinking based on the WQI. The IWQI revealed that 80% of samples were classified as “Excellent” and 16.66% as “Good”. Spatial analysis identified the eastern and southern sections as highly contaminated due to agricultural activities. These findings provide valuable insights for decision-makers to manage groundwater resources and promote sustainable water management in the Gharb region.

**Keywords:** groundwater quality; PIG; NPI; WQI; IWQI; PCA; GIS

## 1. Introduction

Water resources play a pivotal role in fostering economic development and underpinning various socioeconomic sectors [1]. Despite covering about 70% of the Earth’s surface, freshwater—essential for life sustenance—constitutes a mere 3% of the total water available [2]. Groundwater, an indispensable and versatile resource, assumes a crucial

role in supporting diverse human activities. Globally, it stands as the largest and most reliable freshwater source, catering to the drinking water needs of nearly 80% of the world's population [3]. Notably, these groundwater reservoirs represent approximately 23% of the planet's freshwater reserves [4]. Moreover, approximately half of the global drinking water supply and 43% of the water utilized in agriculture are derived from groundwater sources [5].

Globally, in many parts of the world, particularly in arid and semi-arid regions like Morocco, groundwater plays a pivotal role in fulfilling water requirements and forms a significant component of the country's hydraulic heritage, owing to its relatively facile exploitation despite encountering notable challenges [6]. According to previous research, approximately 31% of Morocco's groundwater has been affected by anthropogenic pollution and natural degradation [7]. The confluence of escalating water demands and diminished precipitation resulting from climate change has imposed a considerable strain on groundwater reservoirs within the nation [8]. At the national level, irrigated agriculture accounts for 93% of the total water demand and serves as the primary catalyst for ensuring food security and economic advancement. However, irrigated agriculture in Morocco has been linked to adverse effects on groundwater quality [9–11].

In recent decades, the Gharb Plain has experienced a surge in population, cultural activity, and industrial expansion. Within this Moroccan region, groundwater has emerged as the primary resource to meet escalating water demands across all sectors [12]. Agricultural practices, characterized by their intensity and crop diversity, are identified as potential contributors to water quality degradation in the area. Notably, the groundwater reservoirs of the Gharb are contaminated with organochlorine pesticides, ranging from 0.03 to 0.3 µg/L, attributable to the widespread use of various pesticide varieties in substantial quantities [13]. The excessive application of pesticides, fertilizers, and manure poses significant risks to both consumers of agricultural products and the overall degradation of groundwater quality [14]. The coastal region of Mnasra emerges as the most agriculturally productive area within the Gharb Plain. This region boasts easily accessible groundwater resources, swiftly tapped for irrigation through individual pumping mechanisms. The sheer quantity of wells drilled into the aquifer, surpassing 20,000, underscores its critical agricultural significance [15]. Furthermore, an assessment of pesticide usage in this locality reveals a total application rate of 16.3 Kg/ha, distributed across various categories including 8.8 Kg/ha in nematicides, 4 Kg/ha in insecticides, 2.6 Kg/ha in fungicides, and 0.9 Kg/ha in herbicides [16]. Previous research has demonstrated that agriculture plays a major role in groundwater pollution, representing 60% of the contributing factors [17]. Once groundwater becomes contaminated, restoring its quality by simply halting pollutants at the source is unfeasible. Therefore, the regular monitoring of groundwater quality and the implementation of protective measures are imperative. This alarming scenario has elevated concerns regarding groundwater contamination among researchers, governmental bodies, and environmental organizations [18].

Consequently, there has been increased global attention towards assessing groundwater quality to ensure its suitability for various applications. Various techniques, including binary plots, ionic ratios, Wilcox plots, Piper diagrams, Schoeller diagrams, USSL diagrams, and Gibbs diagrams have been employed to evaluate the hydrogeochemical behavior of groundwater [19–23]. Moreover, to ascertain groundwater suitability, hydrochemical characteristics and ionic concentrations are often assessed against the standards set by the World Health Organization (WHO) [24].

However, comprehensively understanding water quality across various parameters can be challenging. Therefore, to effectively summarize water quality while maintaining its scientific integrity, the WQI method proves invaluable. This approach provides reliable insights into water quality for both ordinary citizens and decision-makers, facilitating ongoing monitoring efforts. For instance, the WQI developed by the work presented in [25] serves as a robust tool for evaluating drinking water quality in any given area, offering a comprehensive assessment of overall water quality. The primary objective of the WQI is to

combine vast datasets encompassing physio-hydrochemical elements and hydrogeological parameters, which exert significant influence on groundwater systems. By converting these complex datasets into quantitative and qualitative water quality data, the WQI enhances our understanding and evaluation of water quality. Calculating the WQI involves a series of computations aimed at synthesizing physicochemical element data into a single value that reflects the validity of water quality for drinking purposes. Furthermore, the PIG serves as an efficient method for assessing groundwater suitability in any given area and conveying comprehensive water quality information [26]. Past research endeavors have evaluated water quality for irrigation purposes by examining key parameters, including the Sodium Adsorption Ratio (SAR), Residual Sodium Carbonate (RSC), Residual Sodium Bicarbonate (RSB), Sodium Percentage (Na%), Permeability Index (PI), Corrosivity Index, Magnesium Hazard (MH), Puri's Salt Index (PSI), Potential Salinity (PS), and Kelly's Ratio (KR) [19,27–30].

To comprehend the factors influencing groundwater quality, MSA have been widely utilized. These include Correlation Analysis (CA), Principal Component Analysis (PCA), and Hierarchical Cluster Analysis (HCA) [21].

In recent years, GIS techniques, coupled with the Inverse Distance Weighting (IDW) interpolation method, have been employed in the assessment and monitoring of groundwater quality [20–23]. This approach has demonstrated its efficacy as a potent tool for evaluating and analyzing spatial information pertaining to water resources. The application of GIS in mapping crucial parameters of groundwater quality significantly influences regional water management strategies and informs future decision-making processes.

The primary objectives of this exploratory study are as follows: firstly, to conduct a comprehensive hydrogeochemical characterization and analysis of the physicochemical properties of groundwater in the Mnasra region within the Gharb Plain; secondly, to assess the groundwater quality utilizing MSA, alongside key indicators including the PIG, NPI, WQI, and IWQI, supplemented by GIS technology; and thirdly, to evaluate water quality specifically for irrigation purposes by considering agricultural indices such as SAR, Na%, RSC, PI, and MH.

## 2. Materials and Methods

### 2.1. Study Area

The Mnasra region, situated within the Gharb plain, is renowned as the most agriculturally productive area along the Atlantic Ocean, spanning an expanse of 488 km<sup>2</sup>. Its boundaries extend from the city of Kenitra in the south to the Sebou River, delineated by a parallel line which passes through Sidi Allal Tazi in the east, and stretches to Merja Zerga near Moulay Bouselham in the north. This region constitutes an integral component of the Gharb-subsidized sedimentary basin, which is nestled in the northwestern part of Morocco. Defined by distinctive geographical and geological attributes, the Gharb Plain is flanked by the Drader-Souier plain to the north and the Maamora plateau to the south, while being bounded by the expansive Atlantic Ocean to the west.

Characterized by a Mediterranean climate with a pronounced oceanic influence, the study area experiences an average annual precipitation of approximately 551 mm. The rainy season generally extends from October to the end of April, peaking during November, December, and January. Temperature variations range from 12 °C during winter to 23 °C in summer. Notably, the potential evaporation exceeds 150 mm per month during the dry months from June to September, whereas it remains below 80 mm from December to February. Elevation levels fluctuate across the region, with the highest point reaching approximately 70 m above sea level (Figure 1).

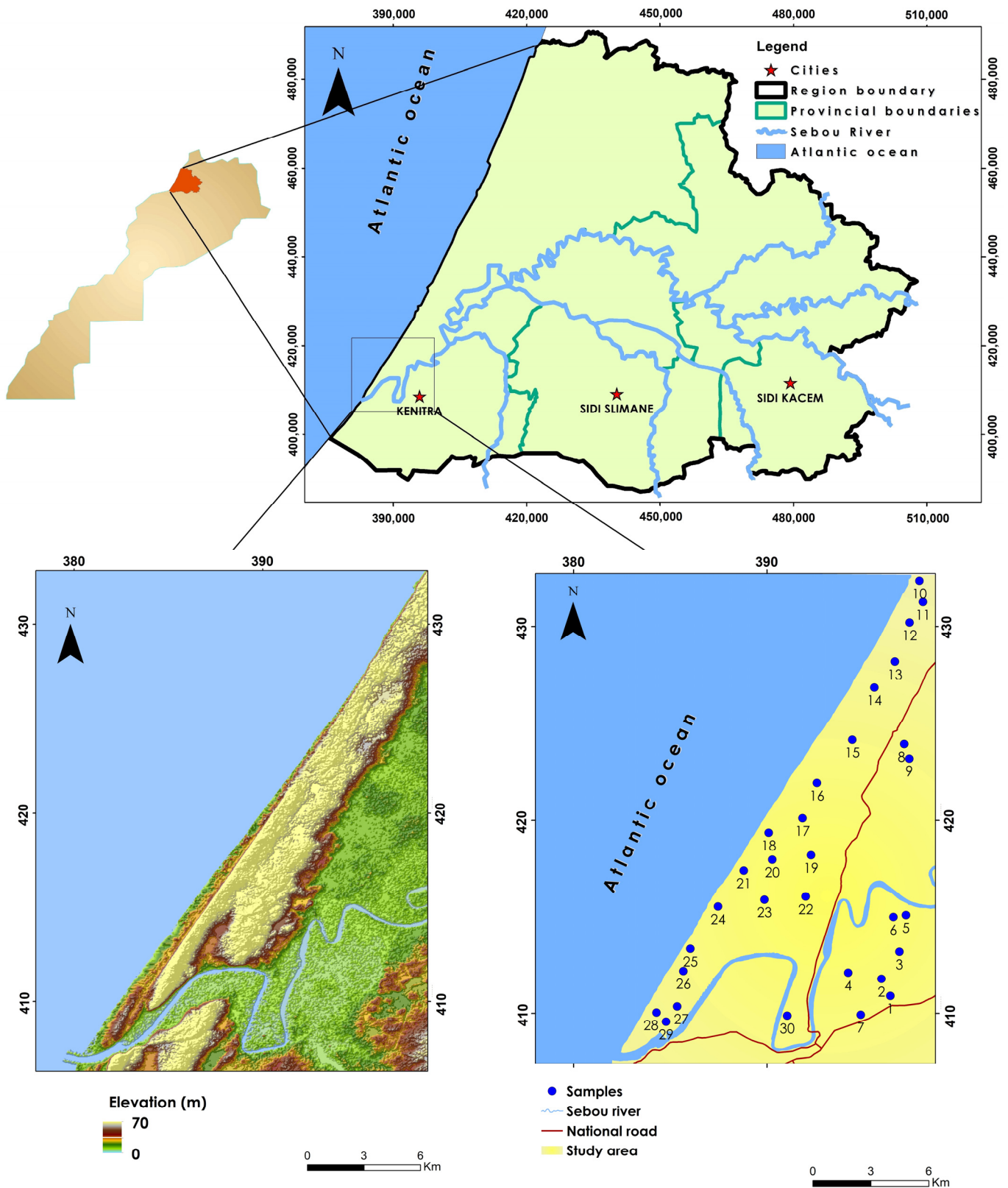


**Figure 1.** Location of the study area and the sampling points.

The hydrological network within the Gharb region is predominantly shaped by the Sebou river, a significant watercourse in the kingdom, along with its tributaries including Ouerrha, Beht, Rdom, and Tiflet.

The geological composition of the Gharb region is characterized by schists and quartzites in the central plain, with a notable impermeable layer of “blue marls” acting as a barrier within the aquifer system [31]. Sedimentation patterns in the area have exhibited a regressive trend since the Pliocene era, marked by the deposition of lumachelles, sandstone, and conglomerates. Along the coastal zone, marine-derived Pelocene sediments, approximately 200 m thick, prevail. These sediments primarily consist of sands, sandstones, and calcareous sandstones, interspersed with thin layers of clayey silt (Figure 2). Sandy soils extensively cover the coastal zone of the Gharb Plain, encompassing around 39,000 hectares or 15% of the total area. These sandy soils significantly influence groundwater recharge and the overall hydrological behavior of the region [15].

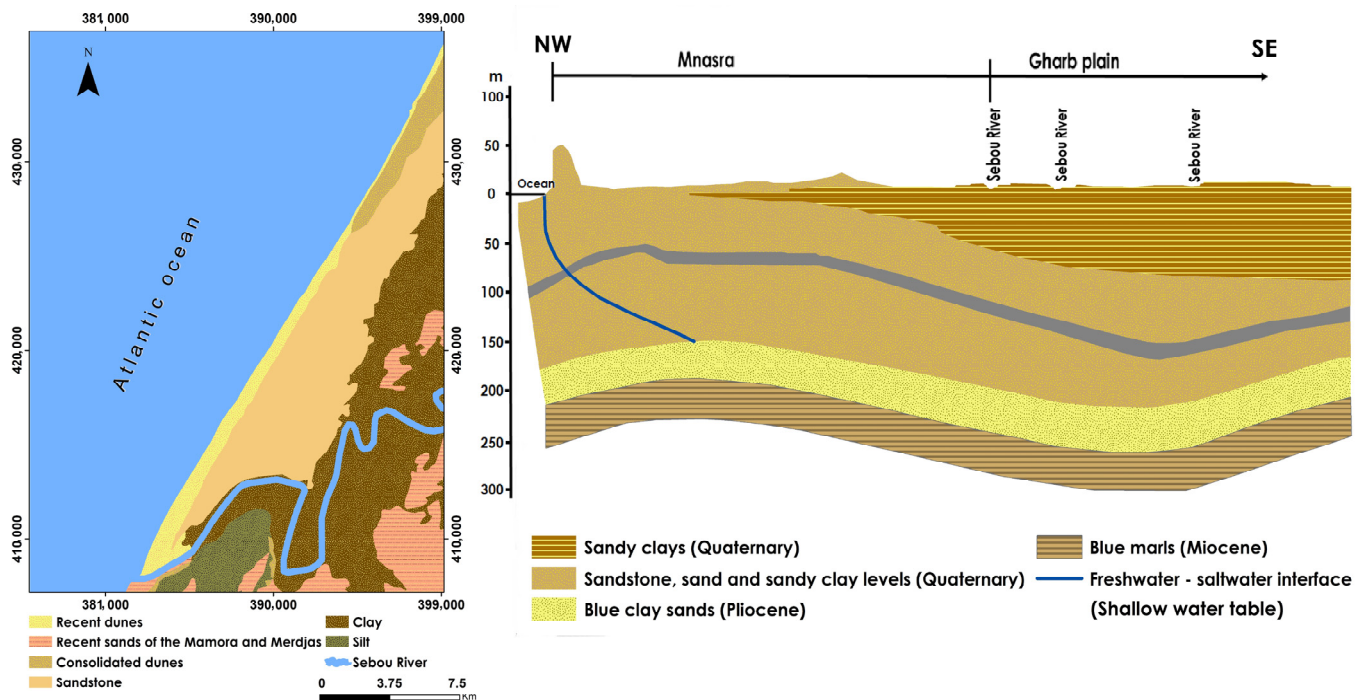


**Figure 2.** Geologic map of the study area.

## 2.2. Sampling Analysis of Groundwater

In November 2023, a total of thirty well samples were carefully collected from various locations within the designated study area, as illustrated in Figure 1, to analyze 23 physicochemical parameters. The sampling sites were selected at regular intervals with minimal deviation, taking into account geographical features and focusing on areas known for intensive agricultural practices and geological importance. The selected wells are used for agricultural and domestic purposes and drinking water. To ensure the accuracy of the collected samples in reflecting the actual groundwater chemistry, the groundwater from the wells was pumped out for more than three minutes prior to sampling. Subsequently, on-site measurements of the Temperature, pH, Electric Conductivity (EC), Salinity (Sal), Total Dissolved Solids (TDS), and Dissolved Oxygen (DO) were conducted using a Portable Multi-parameter Water Quality Meter (Bante 900P Portable pH/Conductivity/Dissolved Oxygen Meter, Multiparameter Water Quality Meter). In situ measurements of these parameters were taken, followed by the immediate filtration of the sampled water through a 45 µm filter. Additionally, the depth of the water level was determined using a two-hundred-meter piezometric sound probe. The sampling procedures adhered strictly to the Standard Methods for the Examination of Water and Wastewater [32]. Following the standards' protocols, precautions were taken to prevent cross-contamination by cleaning the sampling bottles with distilled water before filling and washing them with local sample water three times. Subsequently, the water samples were collected and transported in

portable coolers, maintaining a constant low temperature of 4 °C, to the laboratory for further analysis.

The chemical measurements were conducted in triplicate to ensure the precision of the sample analysis. Potassium (K<sup>+</sup>) and sodium (Na<sup>+</sup>) concentrations were determined using flame photometry, employing the Jenway PFP7 model apparatus. Chlorides (Cl<sup>-</sup>) were quantified using Mohr's method [33]. Calcium (Ca<sup>2+</sup>), magnesium (Mg<sup>2+</sup>), and Total Hardness (TH) levels were measured using the complexometric method with EDTA titration. Carbonate (CO<sub>3</sub><sup>2-</sup>) and bicarbonate (HCO<sub>3</sub><sup>-</sup>) concentrations were determined via titrimetric techniques. Nitrate (NO<sub>3</sub><sup>-</sup>) and ammonium (NH<sub>4</sub><sup>+</sup>) were analyzed through distillation using a distillation apparatus (VELP SCIENTIFICA, Kjeldahl distillation unit, UDK 129). Phosphate (PO<sub>4</sub><sup>3-</sup>) levels were assessed using UV-visible spectrophotometry, specifically the JENWAY 6405 model, at 880 nm. Sulfate (SO<sub>4</sub><sup>2-</sup>) concentrations were determined using the nephelometric method and were measured using a UV-visible colorimeter at 650 nm (JENWAY6405 Model) [33]. Furthermore, concentrations of iron (Fe), zinc (Zn), copper (Cu), and manganese (Mn) were quantified utilizing an atomic absorption spectrophotometer (novAA 800 D Analyzer).

### 2.3. Multivariate Statistical Analysis

Multivariate statistical analyses were performed using IBM SPSS Statistics 25 on a dataset comprising 22 physical-chemical parameters, including (pH), (EC), (TDS), (DO), (K<sup>+</sup>), (Na<sup>+</sup>), (Cl<sup>-</sup>), (Ca<sup>2+</sup>), (Mg<sup>2+</sup>), (TH), (HCO<sub>3</sub><sup>-</sup>), (NO<sub>3</sub><sup>-</sup>), (NH<sub>4</sub><sup>+</sup>), (PO<sub>4</sub><sup>3-</sup>), (SO<sub>4</sub><sup>2-</sup>), (Fe), (Zn), (Cu) and (Mn), which were then subjected to PCA and HCA extraction. Pearson's test was utilized to assess the degree of correlation between the values.

The spatial distribution maps of various physicochemical parameters were generated using GIS techniques and contouring methods with Arc-GIS 10.6. The spatial distribution maps for each parameter were prepared utilizing IDW interpolation techniques to illustrate variations across the study area. Furthermore, the PIG, NPI, WQI, and IWQI were elaborated upon based on these spatial distribution maps.

### 2.4. Groundwater Quality: The Pollution Index of Groundwater (PIG)

The PIG, devised by Subba Rao in 2012 [34], presents a methodological approach to evaluate groundwater quality by assessing the influence of specific variables on its overall quality [35]. This index serves to gauge the relative impact on individual water quality parameters, as detailed in Table 1. The computation of the PIG involves a systematic procedure encompassing five key steps [36].

**Table 1.** The WHO (2017) standards for groundwater quality parameters and the weight values [37].

Parameters	WHO (2017)	Relative Weight (Rw)	Weight Parameter (Wp)
pH	6.5–8.5	4	0.06557
EC	1000 (µs/cm)	5	0.08197
DO	5 (mg/L)	5	0.08197
TDS	500 (mg/L)	2	0.03279
K <sup>+</sup>	10 (mg/L)	3	0.04918
Na <sup>+</sup>	200 (mg/L)	4	0.06557
Cl <sup>-</sup>	250 (mg/L)	4	0.06557
Ca <sup>2+</sup>	75 (mg/L)	3	0.04918
Mg <sup>2+</sup>	50 (mg/L)	3	0.04918
TH	400 (mg/L)	3	0.04918
HCO <sub>3</sub> <sup>-</sup>	120 (mg/L)	2	0.03279
NO <sub>3</sub> <sup>-</sup>	50 (mg/L)	5	0.08197
NH <sub>4</sub> <sup>+</sup>	35 (mg/L)	3	0.04918
PO <sub>4</sub> <sup>3-</sup>	5 (mg/L)	4	0.06557
SO <sub>4</sub> <sup>2-</sup>	250 (mg/L)	4	0.06557

**Table 1.** *Cont.*

Parameters	WHO (2017)	Relative Weight (Rw)	Weight Parameter (Wp)
Fe	0.3 (mg/L)	3	0.04918
Zn	3 (mg/L)	2	0.03279
Cu	2 (mg/L)	1	0.01639
Mn	0.4 (mg/L)	1	0.01639
<b>Total weight</b>		61	1

#### 2.4.1. Assigning Weight Rw

Individual chemical parameters are assigned weights (Rw) ranging from 1 to 5 based on their relative importance in groundwater, as indicated in Table 1.

#### 2.4.2. Weight Parameter Wp

The Weight Parameter (Wp) is calculated using the following Equation (1):

$$W_p = \frac{R_w}{\sum_{i=1}^n R_w} \quad (1)$$

Wp, the weight parameter, is determined based on the Rw, the weight of each constituent, as presented in Table 1.

#### 2.4.3. Status of Concentration Sc

The Status of Concentration (Sc) for each parameter is computed by dividing the concentration of individual chemical variables in each water sample by the corresponding drinking water quality standard [37].

$$S_c = \frac{C}{WQS} \quad (2)$$

#### 2.4.4. Overall Chemical Quality of Water

The overall chemical quality of water (Ow) is determined by Equation (3):

$$O_w = W_p \times S_c \quad (3)$$

Ow, representing the overall chemical quality of water, is calculated using the Wp, the weight parameter, and Sc, the concentration status.

#### 2.4.5. Pollution Index of Ground Water

The groundwater pollution index is derived by summing the Ow values for all parameters analyzed in each water sample.

$$PIG = \sum_{i=1}^n O_w \quad (4)$$

Water classification based on the PIG includes five categories, as outlined in Table 2 [34].

**Table 2.** Classification of the PIG.

PIG Values	PIG Interpretation
Less than 1	Insignificant pollution
From 1 to 1.5	Low pollution
From 1.5 to 2.0	Moderate pollution
From 2 to 2.5	High pollution
Greater than 2.5	Very high pollution

### 2.5. Groundwater Quality: Nitrate Pollution Index (NPI)

Nitrate is a crucial element which significantly impacts groundwater quality, as highlighted in the work presented in [38]. The NPI serves as an index value utilized to assess the extent of nitrate pollution in groundwater. It can be calculated using the following formula Equation (5):

$$NPI = \frac{Cs - HAV}{HAV} \quad (5)$$

where  $C_s$  represents the measured concentration of nitrate in the sample, and HAV denotes the human acceptable value of nitrate, which is typically set at 20 mg/L. Subsequently, the NPI values for all groundwater samples were categorized into one of five classes as presented in Table 3.

**Table 3.** Classification of the NPI.

NPI Values	NPI Interpretation
Less than 0	Clean
From 0 to 1	Light
From 1 to 2	Moderate
From 2 to 3	Significant
Greater than 3	Very significant

### 2.6. Groundwater Quality: Water Quality Index (WQI)

The WQI serves as a crucial parameter in assessing groundwater quality and its suitability for drinking purposes, as outlined in the work presented in [26]. Three consecutive phases are involved in the calculation of the WQI to determine the suitability of drinking water. The initial step involves “assigning weight”, wherein a weight ( $w_i$ ) is assigned to each of the 13 parameters based on their relative importance to drinking water quality compared to the WHO recommendations (2017), as detailed in Table 1. Each criterion receives a specific weight ( $W_i$ ) ranging from 1 (indicating the lowest impact) to 5 (indicating the highest impact). The second step involves calculating the relative weight using the following Equation (6):

$$W_i = \frac{w_i}{\sum_{i=1}^n w_i} \quad (6)$$

The third phase entails the “quality rating ( $Q_i$ )” assessment, which is determined using Equation (7):

$$Q_i = \frac{C_i}{S_i} \times 100 \quad (7)$$

where  $Q_i$  represents the quality index, “ $S_i$ ” denotes the standard norm, and “ $C_i$ ” signifies the concentration of the sample in mg/L. The “ $SI$ ” sub-index for each parameter is computed using the following Formula (8):

$$SI = Q_i \times W_i \quad (8)$$

where “ $Q_i$ ” represents the parameter value, and “ $W_i$ ” signifies the relative weight. The WQI score for each sample is then determined as the sum of all sub-indices computed for all variables using the subsequent Equation (9):

$$WQI = \sum_{i=1}^n SI = \sum_{i=1}^n Q_i \times W_i \quad (9)$$

Subsequently, the WQI scores for all groundwater samples are categorized into one of five water quality classes, as depicted in Table 4 [39].

**Table 4.** Classification of the WQI.

WQI Values	Type of Water
Less than 50	Excellent
From 50 to 100	Good
From 100 to 200	Poor
From 200 to 300	Very poor
Greater than 300	Water unsuitable for drinking

### 2.7. Irrigation Quality: The Irrigation Water Quality Index (IWQI)

In this study, eight indicators were selected for comprehensive analysis to evaluate whether groundwater is suitable for irrigation, containing Electrical Conductivity (EC), Sodium Adsorption Ratio (SAR), Residual Sodium Carbonate (RSC), Sodium Percentage (%Na), Magnesium Adsorption Ratio (MAR), Permeability Index (PI), Residual Sodium Bicarbonate (RSBC), Kelly Ratio (KR), and Potential Salinity (PS) (Table 5).

**Table 5.** Mathematical equations to calculate the IWQ parameters.

IWQ Parameters	Equations	Equation No.
Sodium adsorption ratio	$SAR = \frac{Na^+}{\sqrt{\frac{(Ca^{2+} + Mg^{2+})}{2}}}$	(10)
Residual sodium carbonate	$RSC = [HCO_3^- + CO_3^{2-}] - [Ca^{2+} + Mg^{2+}]$	(11)
Sodium percent	$\%Na = \frac{(Na^+ + K^+) \times 100}{Ca^{2+} + Mg^{2+} + Na^+ + K^+}$	(12)
Magnesium adsorption ratio	$MAR = \frac{Mg^{2+} \times 100}{(Ca^{2+} + Mg^{2+})}$	(13)
Permeability index	$PI = \frac{(\sqrt{HCO_3^- + Na^+}) \times 100}{(Na^+ + Ca^{2+} + Mg^{2+})}$	(14)
Residual sodium bicarbonate	$RSBC = HCO_3^- - Ca^{2+}$	(15)
Kelly ratio	$KR = \frac{Na^+}{Ca^{2+} + Mg^{2+}}$	(16)
Potential salinity	$PS = Cl^- + \frac{1}{2} \times SO_4^{2-}$	(17)

Note: All ionic concentrations are measured in meq/L in all of these Equations (10)–(17).

Electrical Conductivity (EC) serves as a key indicator of salinity hazard, reflecting water quality suitability for irrigation [40].

The Sodium Adsorption Ratio (SAR) indicates the relative activity of Na<sup>+</sup> adsorption in groundwater, predicting Na<sup>+</sup> hazards in high carbonate waters [41]. SAR also serves as an indicator of groundwater alkalization ability, with higher SAR values indicating a stronger alkalization potential.

Residual Sodium Carbonate (RSC) gauges the harmful effects of carbonate and bicarbonate on groundwater quality for irrigation [42]. Elevated levels of carbonate, bicarbonate, calcium, and magnesium in groundwater can affect its suitability for crop cultivation [43].

Sodium concentration, usually expressed as %Na, influences soil permeability and structure [44]. High sodium levels restrict water and airflow in soil, altering its permeability structure and hindering crop growth.

The Magnesium Adsorption Ratio (MAR) values in groundwater contribute to soil alkalinity, resulting in reduced crop productivity. Excessive Mg<sup>2+</sup> levels in irrigation water can impact soil structure and adversely affect crops.

The Permeability Index (PI) assesses water movement capability in soil based on Ca<sup>2+</sup>, Mg<sup>2+</sup>, Na<sup>+</sup>, and HCO<sub>3</sub><sup>-</sup> concentrations [45]. It is a criterion for evaluating water quality suitability for agricultural irrigation, indicating soil permeability and drainage capacity [46].

The Kelly Index (KI) compares sodium to calcium and magnesium levels to determine irrigation water quality. A KI > 1 indicates salt excess, while KI < 2 suggests water deficiency.

Salinity Potential (PS) measures the accumulation of salt in soil due to continuous dissolution in irrigation water, leading to increased salinity.

Irrigation water quality is further classified using an irrigation water classification diagram (USSL and Wilcox diagrams) based on standards from the U.S. Department of Agriculture [47,48]. The USSL diagram illustrates the relationship between EC and SAR, while the Wilcox diagram depicts the relationship between EC and %Na. The IWQI, developed using Equations (6) and (9) with variables EC, SAR, RSC, Na%, MAR, PI, RSBC, KR, and PS, weighs irrigation water quality requirements based on their importance for irrigation, as outlined in Table 6.

**Table 6.** The weight and relative weight of each parameter used for the IWQ calculation.

Parameters	Suitable Limit for Irrigation	Relative Weight (wi)	Weight Parameter (Wi)
EC	2250	5	0.16667
SAR	18	5	0.16667
RSC	2.5	1	0.03333
Na%	60	3	0.10000
MAR	50	3	0.10000
IP	85	4	0.13333
RSBC	5	1	0.03333
KI	1	3	0.10000
PS	5	5	0.16667
<b>Total weight</b>		30	1

Water quality is classified into five categories according to the IWQI values: excellent quality ( $IWQI < 50$ ), good quality ( $50 < IWQI < 100$ ), poor quality ( $100 < IWQI < 200$ ), very poor quality ( $200 < IWQI < 300$ ), and improper quality ( $IWQI > 300$ ).

### 3. Results and Discussion

#### 3.1. Hydrochemical Analysis of Groundwater

Statistical descriptions of various parameters employed to assess the suitability of groundwater for irrigation in the research area are presented in Table 7.

Groundwater temperatures ranged from 17.30 °C to 25.40 °C, averaging 21.57 °C. The measured pH values ranged from 5.00 to 8.40, with a mean of 7.40, indicating a slightly acidic to alkaline nature, mostly falling within the WHO-recommended range of 6.5 to 8.5 (Table 1). However, at locations P3, P5, and P9, pH levels were lower than the drinking water standard of 6.5, as indicated in Table 7.

The Electrical Conductivity (EC) values ranged from 257 to 7330  $\mu\text{S}/\text{cm}$ , with a mean of 891.17  $\mu\text{S}/\text{cm}$ , mostly below the WHO limit of 1000  $\mu\text{S}/\text{cm}$  (Table 1). However, the highest EC values were observed at sites P2, P4, P5, and P7 (Table 7), with spatial analysis revealing values exceeding 750  $\mu\text{S}/\text{cm}$  in the southeast side of the study area (Figure 3). The increased levels of EC in the groundwater at the sampled sites are mainly driven by water–rock interactions, as well as seawater intrusion. These occurrences are especially significant in coastal regions, where seawater intrusion can further elevate EC levels in groundwater [3]. Such increases in EC can hinder water uptake by plants, leading to reduced productivity and yield losses, especially in sensitive crops [49]. The TDS in the groundwater varied from 131.2 to 926 mg/L, with a mean concentration of 276.48 mg/L (Table 7). At two locations, namely P2 and P7 in the southeast side of the study area, the TDS levels exceeded the range recommended by the WHO (Table 1). This could potentially be attributed to interactions between rock and water, as well as agricultural activities in the area. DO concentrations ranged from 3.52 to 15.2 mg/L, with an average of 11.26 mg/L. The majority of samples exhibited DO values above the threshold set by the WHO (Table 1), indicating a well-oxygenated condition in the groundwater. However, a lower DO value was observed at location P12 in the northern part of the study area (Table 7).

**Table 7.** Descriptive statistics and evaluation of physic-chemical parameters.

Samples	T	pH	EC	SAL	TDS	DO	K <sup>+</sup>	Na <sup>+</sup>	Cl <sup>-</sup>	Ca <sup>2+</sup>	Mg <sup>2+</sup>	TH	CO <sub>3</sub> <sup>2-</sup>	HCO <sub>3</sub> <sup>-</sup>	CaCO <sub>3</sub>	NO <sub>3</sub> <sup>-</sup>	NH <sub>4</sub> <sup>+</sup>	PO <sub>4</sub> <sup>3-</sup>	SO <sub>4</sub> <sup>2-</sup>	Fe	Zn	Cu	Mn
P1	18.3	7.33	996	0.47	479	5.23	1.7	26.30	450.85	160.00	26.40	186.40	16.50	33.55	27.50	111.60	23.40	1.85	196.14	0.47	0.19	0.12	0.19
P2	19.7	7.5	1126	0.55	561	14.6	2.3	27.10	692.25	172.00	28.80	200.80	9.00	18.30	15.00	105.40	18.00	1.62	143.07	0.44	0.19	0.18	0.00
P3	17.3	5.5	414	0.13	207	15.17	1	25.00	326.60	36.00	2.40	38.40	9.00	18.30	15.00	99.20	19.80	1.35	7.69	0.41	0.07	0.07	0.00
P4	20.3	8.34	4150	2.15	265	14.11	5.1	27.40	312.40	52.00	88.80	140.80	15.00	30.50	25.00	117.80	21.60	1.88	315.96	0.45	0.19	0.00	0.00
P5	21.7	5	7330	4	355	5.72	2.2	34.30	628.35	172.00	213.60	385.60	36.00	73.20	60.00	161.20	25.20	1.92	432.40	0.41	0.12	0.17	0.00
P6	19.3	8.4	865	0.42	427	14.33	10.9	36.10	450.85	36.00	45.60	81.60	12.00	24.40	20.00	124.00	23.40	1.45	13.69	0.36	0.14	0.00	0.00
P7	20.4	7.17	1853	0.93	926	5.86	2.1	32.80	184.60	260.00	36.00	296.00	10.50	21.35	17.50	148.80	25.20	1.79	88.51	0.39	0.14	0.00	0.00
P8	25.4	7.1	907	0.33	456	12.4	0.6	30.50	390.50	172.00	60.00	232.00	1800	36.60	30.00	111.60	19.80	1.53	82.88	0.38	0.12	0.00	0.00
P9	22.5	5.7	563	0.27	279	7.49	18.8	23.00	220.10	100.00	48.00	148.00	12.00	24.40	20.00	105.40	16.20	0.97	37.69	0.35	0.17	0.00	0.00
P10	22.9	7.47	560	0.27	279	11.72	2.5	24.20	223.65	76.00	72.00	148.00	9.00	18.30	15.00	86.80	14.40	1.51	20.25	0.36	0.26	0.00	0.00
P11	23.9	7.46	599	0.29	299	10.92	1.5	25.10	287.55	80.00	86.40	166.40	15.00	30.50	25.00	80.60	12.60	1.58	13.50	0.35	0.18	0.00	0.00
P12	23.6	7.81	344	0.16	144.4	3.52	1.3	24.50	145.55	84.00	43.20	127.20	6.00	12.20	10.00	74.40	10.80	1.53	2.06	0.36	0.22	0.00	0.00
P13	21.9	7.74	372	0.18	190.4	12.4	1.1	24.20	117.15	64.00	14.40	78.40	9.00	18.30	15.00	74.40	12.60	1.44	10.88	0.34	0.16	0.00	0.00
P14	22.2	6.91	379	0.19	190.4	11.02	1.1	24.40	106.50	64.00	91.20	155.20	10.50	21.35	17.50	68.20	10.80	1.45	6.56	0.33	0.30	0.00	0.00
P15	22.2	7.78	291	0.14	145	12.62	0.8	55.20	88.75	36.00	24.00	60.00	6.00	12.20	10.00	74.40	12.60	1.47	2.25	0.33	0.30	0.00	0.00
P16	22.1	7.88	307	0.15	154.2	12.3	1.8	23.20	81.65	56.00	79.20	135.20	9.00	18.30	15.00	68.20	9.00	1.47	3.56	0.34	0.27	0.00	0.00
P17	19.9	7.66	466	0.17	250	5.87	21.5	18.40	269.80	84.00	14.40	98.40	27.00	54.90	45.00	80.60	12.60	1.44	51.94	0.32	0.31	0.00	0.00
P18	20.6	7.42	450	0.15	230	13.9	21.3	14.70	198.80	76.00	19.20	95.20	10.50	21.35	17.50	62.00	10.80	1.46	41.63	0.32	0.30	0.00	0.00
P19	20.3	7.75	400	0.16	239	15.2	5.1	9.30	184.60	64.00	9.60	73.60	7.50	15.25	12.50	74.40	9.00	1.47	42.19	0.33	0.34	0.00	0.00
P20	20.1	7.65	488	0.19	200	15.12	5.8	8.30	117.15	56.00	4.80	60.80	6.00	12.20	10.00	80.60	14.40	1.30	17.44	0.32	0.39	0.00	0.00
P21	20.9	7.6	463	0.15	231	13.04	35.5	11.00	166.85	60.00	12.00	72.00	12.00	24.40	20.00	55.80	16.20	1.70	14.25	0.32	0.38	0.00	0.00
P22	21.4	7.1	455	0.17	225	13.6	8.1	9.70	188.15	64.00	9.60	73.60	10.50	21.35	17.50	68.20	12.60	1.59	13.69	0.29	0.41	0.00	0.00
P23	21.7	7.6	432	0.16	221	8.6	6.5	8.60	152.65	56.00	9.60	65.60	6.00	12.20	10.00	80.60	16.20	1.57	8.06	0.34	0.40	0.00	0.00
P24	22.6	7.91	261	0.04	192.5	12.63	4.5	6.60	117.15	36.00	14.40	50.40	6.00	12.20	10.00	74.40	12.60	1.58	7.31	0.32	0.43	0.00	0.00
P25	21.4	7.8	270	0.05	154.7	9.09	7.1	6.90	163.30	40.00	24.00	64.00	6.00	12.20	10.00	68.20	7.20	1.68	4.69	0.30	0.52	0.00	0.00
P26	21.6	7.6	335	0.08	163.7	13.05	7.6	3.30	145.55	48.00	31.20	79.20	3.00	6.10	5.00	62.00	16.20	1.63	4.31	0.32	0.51	0.00	0.00
P27	22.1	7.6	294	0.06	146	12.05	5.1	6.00	191.70	48.00	14.40	62.40	7.50	15.25	12.50	80.60	14.40	1.50	5.06	0.33	0.58	0.00	0.00
P28	21.9	7.6	460	0.15	227	13.45	5.4	8.60	181.05	60.00	21.60	81.60	16.50	33.55	27.50	49.60	16.20	1.63	4.69	0.31	0.57	0.00	0.00
P29	24.5	7.85	257	0.05	131.2	11.6	18.7	6.10	145.55	40.00	16.80	56.80	6.00	12.20	10.00	55.80	12.60	1.74	1.13	0.29	0.79	0.00	0.00
P30	24.5	7.65	648	0.26	326	11.32	12.6	17.60	418.90	72.00	19.20	91.20	7.50	15.25	12.50	74.40	14.40	1.57	14.06	0.30	0.70	0.00	0.00
Min	17.30	5.00	257.00	0.04	131.20	3.52	0.60	3.30	81.65	36.00	2.40	38.40	3.00	6.10	5.00	49.60	7.20	0.97	1.13	0.29	0.07	0.00	0.00
Max	25.40	8.40	7330.00	4.00	926.00	15.20	35.50	55.20	692.25	260.00	213.60	385.60	36.00	73.20	60.00	161.20	25.20	1.92	432.40	0.47	0.79	0.18	0.19
MEAN	21.57	7.40	891.17	0.42	276.48	11.26	7.32	19.95	244.95	80.80	39.36	120.16	11.15	22.67	18.58	85.97	15.36	1.56	53.58	0.35	0.32	0.02	0.01
STDV	1.81	0.75	1421.43	0.78	162.99	331	8.22	11.77	154.00	53.18	42.28	78.25	6.75	13.73	11.25	26.79	4.84	0.19	98.97	0.05	0.18	0.05	0.03

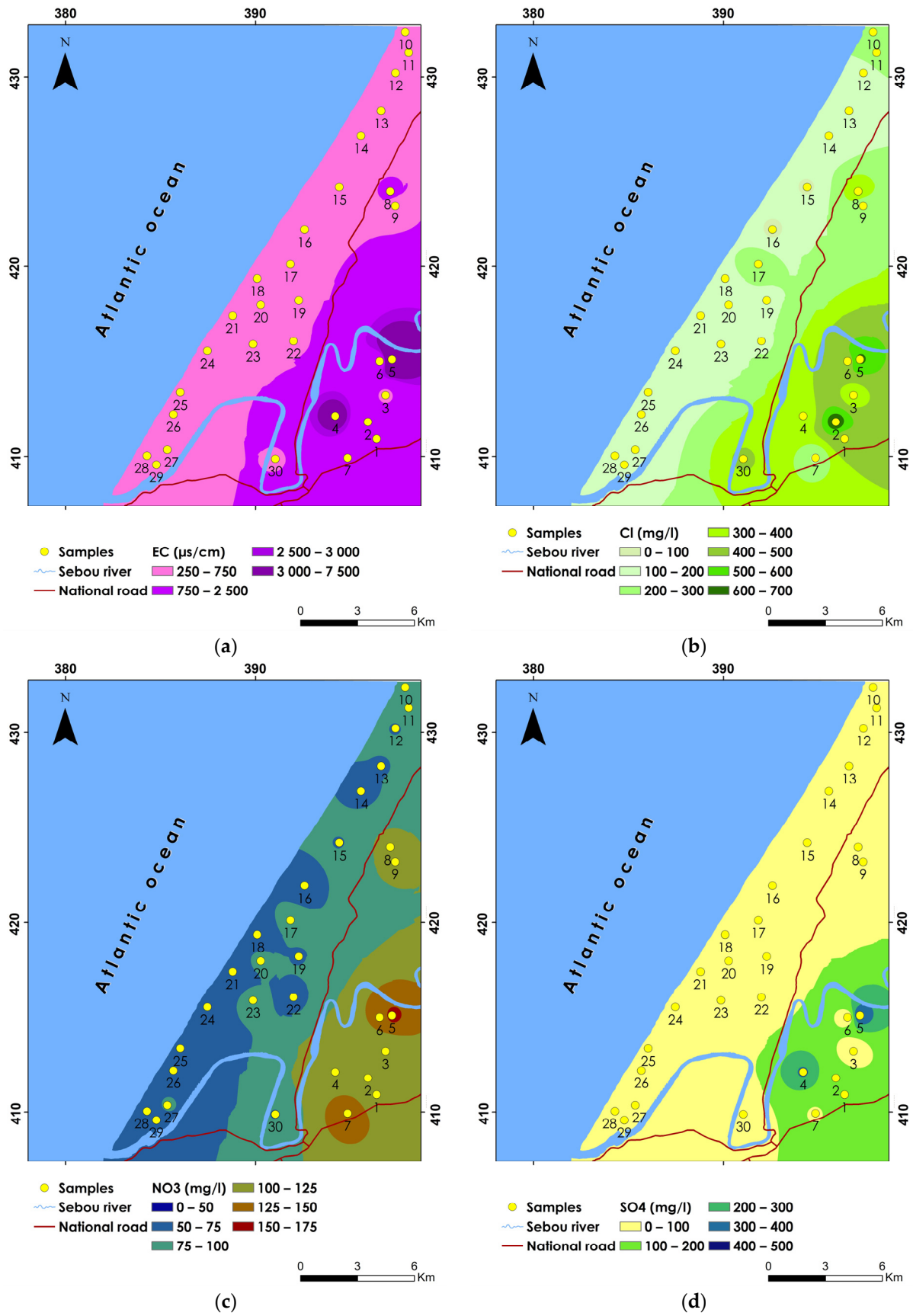


Figure 3. Spatial variation maps of (a) EC, (b) Cl<sup>-</sup>, (c) NO<sub>3</sub><sup>+</sup> and (d) SO<sub>4</sub><sup>2-</sup>.

The concentrations of  $K^+$  and  $Na^+$  in groundwater exhibit a wide range, varying from 0.60 to 35.50 mg/L and from 3.30 to 55.20 mg/L, respectively, with mean values of 7.32 mg/L and 19.95 mg/L (Table 7). While all samples remained below the WHO limit of 200 mg/L for  $Na^+$ , most  $K^+$  concentrations surpassed the WHO threshold of 10 mg/L, except at sites P6, P9, P11, and P12. Although these ions are typically harmless at normal levels, their excess can pose health risks such as hypertension, heart disease, or kidney problems. Excessive  $K^+$  may result in salt transformation and percolation into groundwater, potentially contaminating it, and can induce magnesium deficiencies in crops [3,50]. Sodium in groundwater may originate from geological leaching or silicate rock decomposition, influencing groundwater's electrical conductivity characteristics. Sodium concentrations can vary significantly due to leaching, marine influences, saltwater intrusion, and industrial activities [13]. In irrigation contexts, high sodium concentrations can lead to ion exchange processes in soil, reducing permeability and resulting in poorly drained soil conditions. Chloride ( $Cl^-$ ) values ranged from 81.65 to 692.25 mg/L, with an average of 244.95 mg/L. Elevated chloride levels were observed at multiple locations in the southeast side of the study area (Figure 3), not meeting WHO standards (Table 1). Chlorides in groundwater mainly originate from weathering, salt deposits dissolution, irrigation water infiltration, and agricultural activities, potentially introducing NaCl into groundwater [51]. While chlorides are typically conservative elements in groundwater, their high levels in coastal aquifers may indicate saltwater intrusion [52].

The concentrations of calcium ( $Ca^{2+}$ ) and magnesium ( $Mg^{2+}$ ) in groundwater exhibited a range from 36 to 260 mg/L and 2.4 to 213.6 mg/L, respectively, with mean values of 80.8 mg/L and 39.36 mg/L, respectively. Eleven sites displayed elevated levels of  $Ca^{2+}$  which surpassed the standard value of 75 mg/L, while seven locations recorded high concentrations of  $Mg^{2+}$ , exceeding the standard value of 50 mg/L (Table 7). Although high calcium levels in tap water pose no health risk, they may affect the water's taste. The presence of  $Mg^{2+}$  and  $Ca^{2+}$  in groundwater is attributed to the lithology of the aquifer and the hydrolysis of silicate minerals, which are common constituents of groundwater [53].

Chemical weathering and the erosion of rocks and minerals containing these ions, such as limestone, magnetite, calcite, dolomite, and fluorite, primarily influence the concentrations of  $Mg^{2+}$  and  $Ca^{2+}$  in natural water, significantly contributing to groundwater hardness. All samples exhibited total hardness (TH) values above the WHO threshold of 400 mg/L, ranging from 38.4 to 385.60 mg/L, with a mean value of 120.16 mg/L (Table 7).

Bicarbonate ( $HCO_3^-$ ) and carbonate ( $CO_3^{2-}$ ) proportions regulate alkalinity in water. The concentrations of  $CO_3^{2-}$  and  $HCO_3^-$  ranged from 3 to 36 mg/L and 6.1 to 73.2 mg/L, respectively, with average values of 11.15 mg/L and 22.67 mg/L (Table 7). None of the samples exceeded the drinking water standard limit for these ions.

The concentrations of nitrate ( $NO_3^-$ ) and ammonium ( $NH_4^+$ ) in groundwater varied between 49.6 to 161.2 mg/L and 7.2 to 25.2 mg/L, respectively, with mean values of 85.97 mg/L and 15.36 mg/L, respectively (Table 7). All samples exceeded the WHO standard for  $NO_3^-$  set at 50 mg/L, while concentrations of  $NH_4^+$  in all groundwater samples were above the WHO threshold of 35 mg/L (Table 1).  $NO_3^-$  are natural components of the nitrogen cycle, primarily originating from fertilizers and organic waste, absorbed by plants during growth for nitrogen compound synthesis. Excessive nitrate production disrupts this cycle, leading to soil nitrate accumulation and migration into water resources, with intensive agricultural practices and livestock farming major contributors to nitrate pollution [54,55].

Phosphate ( $PO_4^{3-}$ ) concentrations in groundwater remained low, not exceeding the WHO standard of 5 mg/L, with measured concentrations ranging from 0.97 to 1.92 mg/L and an average value of 1.56 mg/L (Table 7). However, most samples exceeded the WHO threshold for sulfate ( $SO_4^{2-}$ ) at 250 mg/L (Table 1), with sites P4 and P5 recording elevated values of 315.96 mg/L and 432.40 mg/L, respectively.  $SO_4^{2-}$  concentrations ranged from 1.13 to 432.4 mg/L, with a mean value of 53.58 mg/L (Table 7), naturally occurring and closely associated with major cations such as  $Ca^{2+}$ ,  $Mg^{2+}$ , and  $Na^+$  [3]. Additionally,

urban pollution, industrial activities, and agricultural practices can introduce sulfates into groundwater [56].

In the groundwater samples analyzed, concentrations of iron (Fe) ranged from 0.29 to 0.47 mg/L, while zinc (Zn) concentrations varied from 0.07 to 0.79 mg/L, with mean values of 0.35 mg/L and 0.32 mg/L, respectively (Table 7). Specifically, sites P22, P25, P29, and P30 exhibited minimum iron concentrations, measuring 0.29, 0.30, 0.29, and 0.30 mg/L, respectively, all below the standard value of 0.3 mg/L. Zinc levels in all sites remained below the WHO standard of 3 mg/L (Table 1). Iron in groundwater is primarily derived from the weathering of iron-bearing minerals and rocks, occurring naturally in the reduced  $\text{Fe}^{2+}$  state within the aquifer. Its dissolution leads to increased concentrations in groundwater. Additionally, the concentrations of copper (Cu) and manganese (Mn) in the analyzed samples were notably low, with average concentrations of 0.02 mg/L and 0.01 mg/L, respectively.

### 3.2. Correlation Coefficient Matrix Analysis

Correlation analysis serves as a fundamental statistical approach in water quality studies, offering insights into the inter-relationships among different ions and their influence on water chemistry [57]. Essentially, it quantifies the degree to which one variable predicts changes in another. The correlation matrix, as described in the work presented in [58], is a statistical tool used to assess the associations between physiochemical variables in groundwater. A correlation coefficient ( $r$ ) close to +1 or  $-1$  indicates a strong positive or negative correlation, respectively, between two variables. Conversely, an  $R$ -value near zero suggests a weak or nonexistent correlation [59]. In practice, correlations with  $R$ -values exceeding 0.7 are considered high, while those falling between 0.5 and 0.7 indicate moderate correlations [60].

The results of a Pearson correlation matrix obtained from the statistical analysis of 22 selected variables are presented in Table 8.

The correlation matrix analysis reveals significant relationships among various ions in groundwater, shedding light on the underlying processes influencing water chemistry [21]. Notably, a strong positive correlation ( $r = 0.703$ ) between EC and TDS suggests that water conductivity is influenced by total dissolved solids (TDS), indicating the dominance of mineral dissolution, solubility, ion exchange, and anthropogenic activities in shaping groundwater chemistry. Moreover, positive correlations were observed between EC and TDS with several ions including  $\text{Na}^+$ ,  $\text{Cl}^-$ ,  $\text{Ca}^{2+}$ ,  $\text{Mg}^{2+}$ ,  $\text{CO}_3^{2-}$ ,  $\text{HCO}_3^-$ ,  $\text{NO}_3^-$ ,  $\text{NH}_4^+$ ,  $\text{PO}_4^{3-}$ ,  $\text{SO}_4^{2-}$ , Fe, and Cu, underscoring their role in controlling groundwater chemistry. The presence of  $\text{Na}^+$  and  $\text{Cl}^-$  ions, often associated with saline intrusion or anthropogenic activities, can elevate both EC and TDS levels. Similarly, the dissolution of carbonate and bicarbonate minerals in the aquifer can increase these parameters due to the release of ions such as  $\text{Ca}^{2+}$  and  $\text{HCO}_3^-$ . Additionally, the presence of nutrients like  $\text{NO}_3^-$  and  $\text{NH}_4^+$  from agricultural activities or sewage contamination can also impact EC and TDS levels. Furthermore, a notable positive correlation ( $r = 0.835$ ) between  $\text{Ca}^{2+}$  and  $\text{Mg}^{2+}$  suggests their common source from carbonate minerals like calcite and dolomite [61]. This finding is supported by a high correlation ( $r > 0.8$ ) between  $\text{Ca}^{2+}$ ,  $\text{Mg}^{2+}$ , and TH, indicating that water hardness is primarily defined by the combined concentration of calcium and magnesium ions. Moreover, the strong relationship ( $r = 0.820$ ) between  $\text{NH}_4^+$  and  $\text{NO}_3^-$  suggests that low  $\text{NH}_4^+$  concentrations in groundwater may be attributed to their interdependence. Conversely, the association between  $\text{SO}_4^{2-}$  and Fe ( $r > 0.7$ ) may indicate anthropogenic contamination, possibly from agricultural or domestic sources [62].

Additionally, a high positive correlation ( $r > 0.7$ ) between  $\text{NO}_3^-$  and  $\text{SO}_4^{2-}$  suggests groundwater contamination from excessive fertilizer use. Furthermore, the high correlation ( $r = 0.760$ ) between  $\text{Na}^+$  and  $\text{Cl}^-$  highlights the influence of irrigation practices, evaporation, and coastal activities on aquatic ecosystems [63].

**Table 8.** Pearson correlation matrix of the water parameters.

	pH	EC	SAL	TDS	DO	K <sup>+</sup>	Na <sup>+</sup>	Cl <sup>-</sup>	Ca <sup>2+</sup>	Mg <sup>2+</sup>	TH	CO <sub>3</sub> <sup>2-</sup>	HCO <sub>3</sub> <sup>-</sup>	CaCO <sub>3</sub>	NO <sub>3</sub> <sup>-</sup>	NH <sub>4</sub> <sup>+</sup>	PO <sub>4</sub> <sup>3-</sup>	SO <sub>4</sub> <sup>2-</sup>	Fe	Zn	Cu	Mn	
pH	1																						
EC	-0.436	1																					
SAL	-0.442	0.999	1																				
TDS	-0.142	0.703	0.695	1																			
DO	0.264	-0.256	-0.267	-0.257	1																		
K <sup>+</sup>	0.079	-0.162	-0.174	-0.158	0.031	1																	
Na <sup>+</sup>	-0.197	0.349	0.367	0.403	-0.190	-0.358	1																
Cl <sup>-</sup>	-0.334	0.560	0.554	0.519	-0.087	-0.108	0.760	1															
Ca <sup>2+</sup>	-0.363	0.432	0.428	0.872	-0.481	-0.210	0.379	0.513	1														
Mg <sup>2+</sup>	-0.436	0.800	0.814	0.146	-0.306	-0.285	0.434	0.405	0.835	1													
TH	-0.482	0.726	0.731	0.671	-0.492	-0.297	0.492	0.567	0.861	0.868	1												
CO <sub>3</sub> <sup>2-</sup>	-0.467	0.703	0.702	0.269	-0.384	0.064	0.320	0.549	0.443	0.644	0.649	1											
HCO <sub>3</sub> <sup>-</sup>	-0.467	0.703	0.702	0.269	-0.384	0.064	0.320	0.549	0.443	0.644	0.649	1.000	1										
CaCO <sub>3</sub>	-0.467	0.703	0.702	0.269	-0.384	0.064	0.320	0.549	0.443	0.644	0.649	1.000	1.000	1									
NO <sub>3</sub> <sup>-</sup>	-0.440	0.723	0.722	0.719	-0.342	-0.313	0.581	0.652	0.693	0.550	0.768	0.533	0.533	0.533	1								
NH <sub>4</sub> <sup>+</sup>	-0.346	0.604	0.591	0.687	-0.172	-0.121	0.417	0.629	0.581	0.334	0.575	0.465	0.465	0.465	0.820	1							
PO <sub>4</sub> <sup>2-</sup>	0.159	0.531	0.517	0.300	-0.199	-0.109	0.005	0.308	0.323	0.318	0.391	0.291	0.291	0.291	0.246	0.377	1						
SO <sub>4</sub> <sup>2-</sup>	-0.366	0.934	0.929	0.369	-0.266	-0.170	0.350	0.655	0.514	0.693	0.724	0.700	0.700	0.700	0.725	0.629	0.565	1					
Fe	-0.284	0.533	0.531	0.546	-0.203	-0.387	0.542	0.649	0.561	0.377	0.585	0.364	0.364	0.364	0.748	0.713	0.310	0.706	1				
Zn	0.373	-0.345	-0.357	-0.438	0.164	0.333	-0.682	-0.358	-0.458	-0.396	-0.526	-0.387	-0.387	-0.387	-0.651	-0.447	0.129	-0.399	-0.699	1			
Cu	-0.485	0.540	0.545	0.361	-0.157	-0.245	0.286	0.799	0.501	0.382	0.547	0.438	0.438	0.438	0.523	0.488	0.347	0.658	0.678	-0.351	1		
Mn	-0.017	0.014	0.013	0.235	-0.344	-0.129	0.102	0.253	0.281	-0.058	0.160	0.150	0.150	0.150	0.181	0.314	0.298	0.272	0.472	-0.138	0.378	1	

### 3.3. Principal Component Analysis (PCA)

PCA serves as a valuable statistical tool in analyzing complex datasets containing a multiple of parameters with wide-ranging data. In PCA, the principal component loadings are categorized as strong, moderate, or weak, based on their absolute loading values: values exceeding 0.75 indicate strong loadings, those between 0.75 and 0.50 signify moderate loadings, and values ranging from 0.50 to 0.30 represent weak loadings [64]. In our study, PCA was applied to 22 physicochemical parameters, resulting in the identification of five principal components that collectively explain 85.03% of the total variance in the data (Table 9). Notably, the PC1—PC2 combination accounts for over 60.14% of the dataset's variability (Figure 4), suggesting that the chemical evolution of groundwater is predominantly captured within these two components.

**Table 9.** The correlation between the principal components and physicochemical and parameters.

Parameters	Components					
	PC1	PC2	PC3	PC4	PC5	PC6
pH	−0.525	0.161	0.391	0.190	−0.260	−0.117
EC	0.858	−0.322	0.050	0.314	−0.091	−0.084
SAL	0.859	−0.321	0.028	0.315	−0.100	−0.064
TDS	0.606	0.542	0.137	−0.265	−0.143	−0.436
DO	−0.415	0.046	−0.080	0.555	0.463	−0.346
K <sup>+</sup>	−0.251	−0.437	0.227	−0.454	0.308	−0.395
Na <sup>+</sup>	0.550	0.333	−0.454	0.074	−0.094	0.063
Cl <sup>−</sup>	0.745	0.116	0.167	0.072	0.429	−0.111
Ca <sup>2+</sup>	0.730	0.357	0.092	−0.350	−0.230	−0.191
Mg <sup>2+</sup>	0.733	−0.356	−0.242	0.258	−0.272	0.117
TH	0.892	0.050	−0.068	−0.098	−0.304	−0.067
CO <sub>3</sub> <sup>2−</sup>	0.790	−0.473	−0.045	−0.249	0.101	0.041
HCO <sub>3</sub> <sup>−</sup>	0.790	−0.473	−0.045	−0.249	0.101	0.041
CaCO <sub>3</sub>	0.790	−0.473	−0.045	−0.249	0.101	0.041
NO <sub>3</sub> <sup>−</sup>	0.874	0.265	−0.128	0.030	−0.038	−0.187
NH <sub>4</sub> <sup>+</sup>	0.756	0.276	0.154	0.005	0.162	−0.275
PO <sub>4</sub> <sup>3−</sup>	0.443	−0.091	0.718	0.268	−0.305	−0.011
SO <sub>4</sub> <sup>2−</sup>	0.891	−0.167	0.196	0.247	0.033	0.047
Fe	0.758	0.464	0.045	0.162	0.192	0.163
Zn	−0.602	−0.361	0.534	0.041	−0.096	−0.086
Cu	0.701	0.147	0.192	0.137	0.403	0.213
Mn	0.279	0.360	0.489	−0.272	0.158	0.576
Eigenvalue	10.778	2.453	1.702	1.469	1.213	1.091
Variability (%)	48.992	11.150	7.737	6.679	5.516	4.959
Cumulative	48.992	60.142	67.879	74.558	80.073	85.033

The PC1 contributes significantly to the overall variance, explaining 48.99% of the overall variation, whereas PC2 represents 10.89% of the total variability. These components are typically linked to anthropogenic contamination, resulting from agricultural activities in the research area. The PC1 demonstrates large positive loadings for parameters such as EC, SAL, Cl<sup>−</sup>, Ca<sup>2+</sup>, Mg<sup>2+</sup>, TH, HCO<sub>3</sub><sup>−</sup>, CO<sub>3</sub><sup>2−</sup>, CaCO<sub>3</sub>, NO<sub>3</sub><sup>−</sup>, NH<sub>4</sub><sup>+</sup>, SO<sub>4</sub><sup>2−</sup>, Fe, and Cu. The results indicate that PC1 mainly reflects the mineralization and ion content of groundwater, influenced by natural geological processes and human activities like agricultural runoff and industrial discharge. Notably, PC1 shows moderate loadings for TDS and Na<sup>+</sup>. Surprisingly, pH shows negative correlations with most parameters, suggesting an inverse relationship between pH and the presence of ions and minerals in groundwater. Lower pH values are associated with higher mineralization and salinity levels. The PC3 is characterized by a high positive loading for PO<sub>4</sub><sup>2−</sup>, indicating its influence on water quality variability. PO<sub>4</sub><sup>2−</sup> levels in groundwater can be attributed to agricultural practices, such as fertilizer application, and sewage contamination. In contrast,

PC4 explains the variance associated with  $K^+$  and DO. The high positive loading for  $K^+$  suggests its contribution to groundwater variability, possibly originating from natural weathering processes or agricultural activities. Finally, the PC6 explains the variance related to Mn, highlighting its contribution to groundwater quality variability. Elevated manganese levels can result from both natural sources and anthropogenic inputs, such as industrial discharges and agricultural practices.

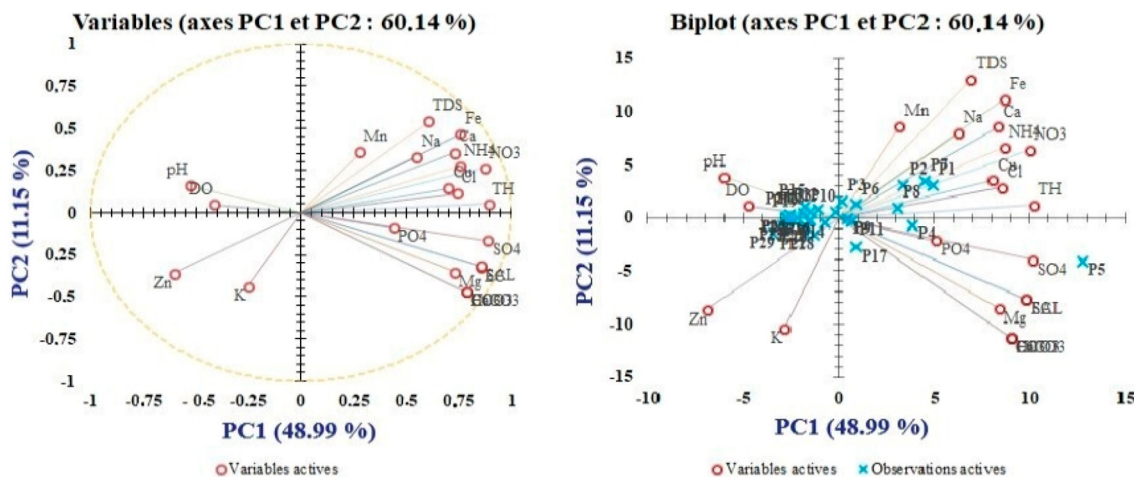


Figure 4. Principal component analysis of the principal groundwater parameters.

### 3.4. Hierarchical Cluster Analysis (HCA)

As part of our research, HCA was employed to delineate between distinct groundwater groups based on their physicochemical characteristics. HCA ensures that each cluster exhibits homogeneity in specific qualities while being distinguishable from other clusters based on the same characteristics. The dendrogram, a graphical representation, was utilized to determine the number of homogeneous units and illustrate the proximity of the groups. In this study, the [65] linkage method with a Euclidean distance was employed to conduct HCA, as described in previous research [7]. The analysis revealed the classification of groundwater samples into four clusters according to their physicochemical attributes (Figure 5).

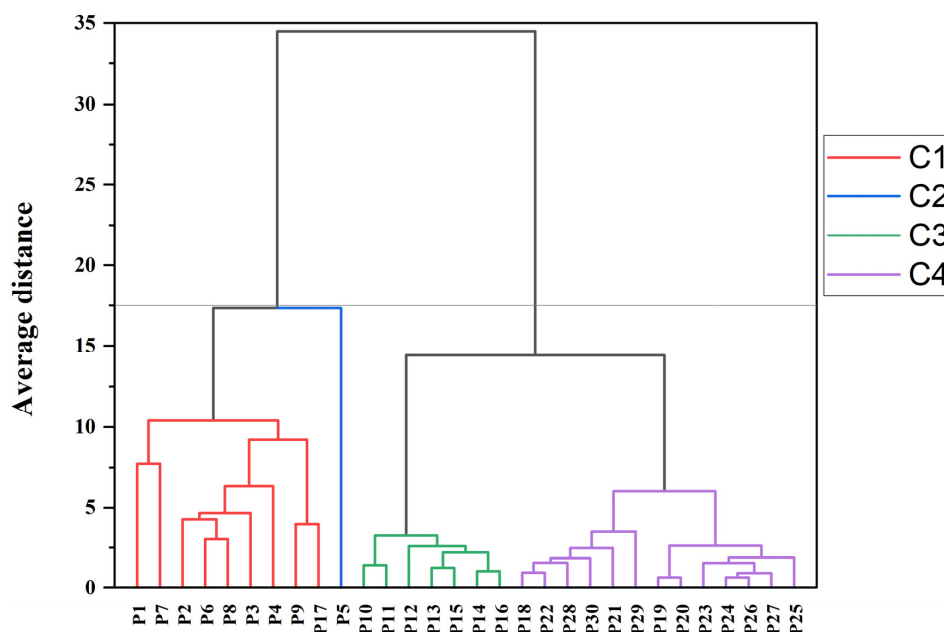


Figure 5. Dendrogram of the groundwater samples.

Cluster 1 comprised two sub-clusters. The first sub-cluster consisted of samples P1 and P2, while the second sub-cluster included seven samples (P2, P6, P8, P3, P4, P9, and P17). These samples exhibited elevated levels of various parameters such as EC, TDS,  $K^+$ ,  $Na^+$ ,  $Cl^-$ ,  $Ca^{2+}$ ,  $Mg^{2+}$ , TH,  $NO_3^-$ ,  $NH_4^+$ ,  $PO_4^{3-}$ ,  $SO_4^{2-}$ , and Fe.

In contrast, Cluster 2 consisted of a single sample (P5) characterized by the highest concentrations of EC, SAL,  $Cl^-$ ,  $Ca^{2+}$ ,  $Mg^{2+}$ , TH,  $CO_3^{2-}$ ,  $HCO_3^-$ ,  $CaCO_3$ ,  $NO_3^-$ ,  $NH_4^+$ ,  $PO_4^{3-}$  and  $SO_4^{2-}$ . The distribution of samples in Clusters 1 and 2, primarily located in the southeast side of the Mnasra region, suggests the influence of agricultural activities and intensive fertilizer usage in this area.

Cluster 3 encompassed seven samples (P10, P11, P12, P13, P14, P15, P16) located in the northwestern side of the study area, exhibiting medium mineralization levels lower than those in Clusters 1 and 2.

Cluster 4 comprised thirteen samples (P18, P19, P20, P21, P22, P23, P24, P25, P26, P27, P28, P29, and P30) found in the western and southwest portions of the study area, indicating weak mineralization. Overall, the southeastern part of the study area exhibited the highest mineralization compared to other coastal regions (northwestern, western, southwest). This multivariate statistical approach involving PCA and HCA suggests that water–rock interactions, agricultural activities, and irrigation systems are the primary sources of pollution. Further investigation utilizing index methods will refine and validate these hypotheses in the subsequent sections of our study.

### 3.5. Groundwater Type: Piper Diagram

In assessing groundwater chemistry, hydrochemical facies play an essential role in determining the interactions between the main anions and cations and their behavior. This classification makes it possible to identify the origin and categorization of different types of water [23]. Piper introduced a trilinear diagram, a widely utilized tool in hydrogeology, to depict the geochemical evolution of groundwater [66]. This diagram comprises two triangular plots at the base, representing major cations and anions, and a diamond-shaped plot at the apex symbolizing the chemistry of water samples. To determine the hydro-geochemical facies of groundwater, we utilized the concentrations of major anions ( $Cl^-$ ,  $SO_4^{2-}$ ,  $NO_3^-$  and  $HCO_3^-$ ) and cations ( $Ca^{2+}$ ,  $Mg^{2+}$ ,  $Na^+$ , and  $K^+$ ) in meq/L, plotted on the Piper diagram as illustrated in (Figure 6). The diagram delineates six distinct water types, including  $Ca^{2+}$ - $HCO_3^-$ ,  $Na^+$ - $Cl^-$ , mixed  $Ca^{2+}$ - $Na^+$ - $HCO_3^-$ , mixed  $Ca^{2+}$ - $Mg^{2+}$ - $Cl^-$ ,  $Ca^{2+}$ - $Cl^-$ , and  $Na^+$ - $HCO_3^-$  types.

Upon critical evaluation of the diagram, all samples were categorized under the calcium–chloride facies, indicative of a predominant  $Ca^{2+}$ - $Cl^-$  water type, hinting at the hypothesis of groundwater interaction with saline waters. The distribution of samples towards the chloride pole on the anions triangle suggests the potential influence of seawater intrusion [7].

In terms of cations, calcium ( $Ca^{2+}$ ) emerged as the dominant ion in 56.66% of samples, followed by magnesium ( $Mg^{2+}$ ) at 20%, with 23.33% showing no dominance. Sources of calcium in water encompass various minerals such as calcite, dolomite, gypsum, and others [3]. Multiple studies have highlighted the impact of diverse factors, including agricultural activities (such as irrigation return flows and chemical fertilizer usage), natural processes such as water–rock interactions, and mixing with marine waters on water types [9,23,38].

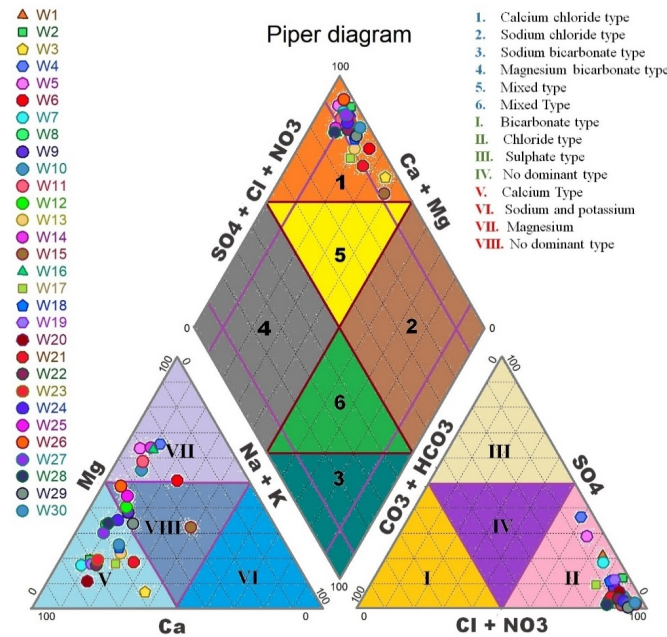


Figure 6. Piper trilinear diagram of the analyzed samples.

### 3.6. Groundwater Type: Gibbs Diagram

The Gibbs diagram, introduced by the work presented in [67], offers insights into the chemical dynamics of water and its interactions within the subsurface environment, particularly with various rock lithologies. This classification system comprises three main types: Type-I, characterized by evaporation dominance driven by the rate of surface and subsurface evaporation; Type-II, exhibiting rock dominance attributed to the chemical weathering of rocks by water; and Type-III, indicating precipitation dominance resulting from surface or subsurface precipitation.

In Figure 7, the Gibbs plot for anions and cations is presented. Notably, all groundwater samples fall within the field of rock dominance, underscoring the significant role of rock weathering and water–rock interactions in shaping the chemistry of groundwater in both plots. This observation suggests that the concentrations of sodium and the ratio of calcium to sodium may experience augmentation due to the leaching of salts from rocks, thereby contributing to the overall chemical composition of groundwater.

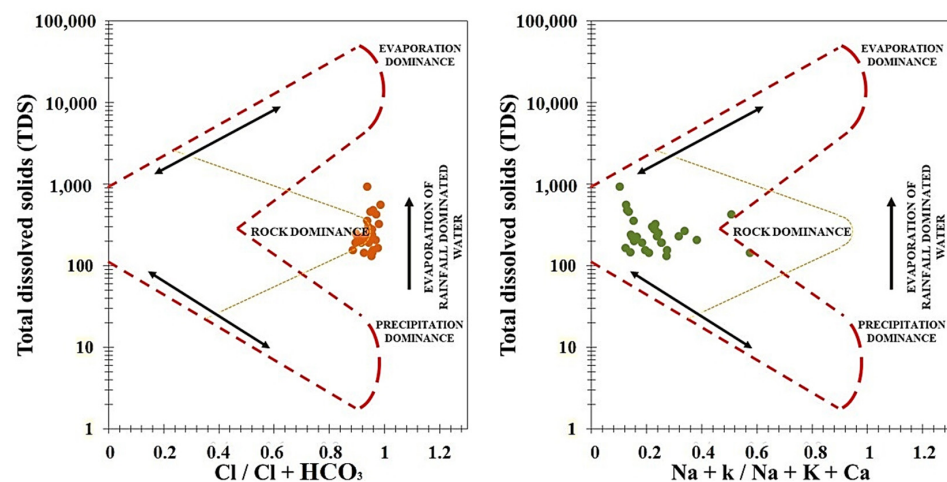


Figure 7. The Gibbs diagram illustrates the mechanism that controls groundwater chemistry.

### 3.7. Pollution Index of Groundwater (PIG)

The PIG serves as a comprehensive metric, considering the collective impact of various chemical variables on groundwater quality, thus providing a singular value indicative of the overall groundwater pollution rate [68]. The calculated PIG values, outlined in Table 10, ranged from 0.51 to 1.92, delineating the water quality into three distinct categories: “Insignificant pollution”, “low pollution”, and “moderate pollution”.

**Table 10.** Water quality classifications of samples based on the PIG, NPI, WQI, and IWQI values.

Samples	PIG Value	Class	NPI Value	Class	WQI Value	Class	IWQI Value	Class
P1	0.91	Insignificant pollution	4.58	Very significant	87.60	Good	49.67	Excellent
P2	1.11	Low pollution	4.27	Very significant	107.42	Poor	68.72	Good
P3	0.81	Insignificant pollution	3.96	Very significant	71.07	Good	53.84	Good
P4	1.26	Low pollution	4.89	Very significant	125.89	Poor	78.73	Good
P5	1.92	Moderate pollution	7.06	Very significant	180.46	Poor	108.18	Poor
P6	0.93	Insignificant pollution	5.2	Very significant	92.19	Good	68.08	Good
P7	1.06	Low pollution	6.44	Very significant	101.86	Poor	13.63	Excellent
P8	0.99	Insignificant pollution	4.58	Very significant	94.93	Good	36.90	Excellent
P9	0.85	Insignificant pollution	4.27	Very significant	76.14	Good	27.50	Excellent
P10	0.76	Insignificant pollution	3.34	Very significant	72.89	Good	29.03	Excellent
P11	0.77	Insignificant pollution	3.03	Very significant	73.83	Good	34.05	Excellent
P12	0.51	Insignificant pollution	2.72	Significant	48.42	Excellent	19.58	Excellent
P13	0.60	Insignificant pollution	2.72	Significant	57.99	Good	23.53	Excellent
P14	0.68	Insignificant pollution	2.41	Significant	62.82	Good	16.86	Excellent
P15	0.58	Insignificant pollution	2.72	Significant	56.13	Good	37.12	Excellent
P16	0.63	Insignificant pollution	2.41	Significant	61.38	Good	16.24	Excellent
P17	0.70	Insignificant pollution	3.03	Very significant	66.90	Good	37.72	Excellent
P18	0.77	Insignificant pollution	2.1	Significant	73.07	Good	28.54	Excellent
P19	0.69	Insignificant pollution	2.72	Significant	66.20	Good	25.59	Excellent
P20	0.67	Insignificant pollution	3.03	Very significant	64.69	Good	19.49	Excellent
P21	0.78	Insignificant pollution	1.79	Moderate	75.34	Good	28.28	Excellent
P22	0.69	Insignificant pollution	2.41	Significant	64.00	Good	26.40	Excellent
P23	0.59	Insignificant pollution	3.03	Very significant	56.13	Good	22.97	Excellent
P24	0.58	Insignificant pollution	2.72	Significant	56.29	Good	23.30	Excellent
P25	0.54	Insignificant pollution	2.41	Significant	52.23	Good	26.96	Excellent
P26	0.64	Insignificant pollution	2.1	Significant	60.75	Good	21.59	Excellent
P27	0.63	Insignificant pollution	3.03	Very significant	60.05	Good	27.08	Excellent
P28	0.64	Insignificant pollution	1.48	Moderate	61.35	Good	27.50	Excellent
P29	0.61	Insignificant pollution	1.79	Moderate	59.37	Good	25.65	Excellent
P30	0.77	Insignificant pollution	2.72	Significant	74.32	Good	50.40	Good

An analysis of the results reveals that a significant majority, approximately 86.66% of the wells, fall within the “Insignificant pollution” category ( $PIG < 1$ ), signifying excellent suitability for rural consumption. Conversely, around 10% of the wells, specifically P2, P4, and P7, are classified as experiencing “low pollution” ( $1 < PIG < 1.5$ ). Notably, the highest PIG value of 1.92 was recorded at P5, attributed to its exposure to anthropogenic activities, thus categorizing it as “moderate pollution” ( $1.5 < PIG < 2$ ).

The spatial distribution of PIG values, depicted in (Figure 8a), elucidates the geographical variation in groundwater pollution. Specifically, samples collected from the northwest, western, and southwest regions of the study area exhibit “Insignificant pollution”, whereas the southeast part of the Mnasra region demonstrates “moderate pollution”, attributed to agricultural practices, excessive fertilizer usage, and geological attributes.

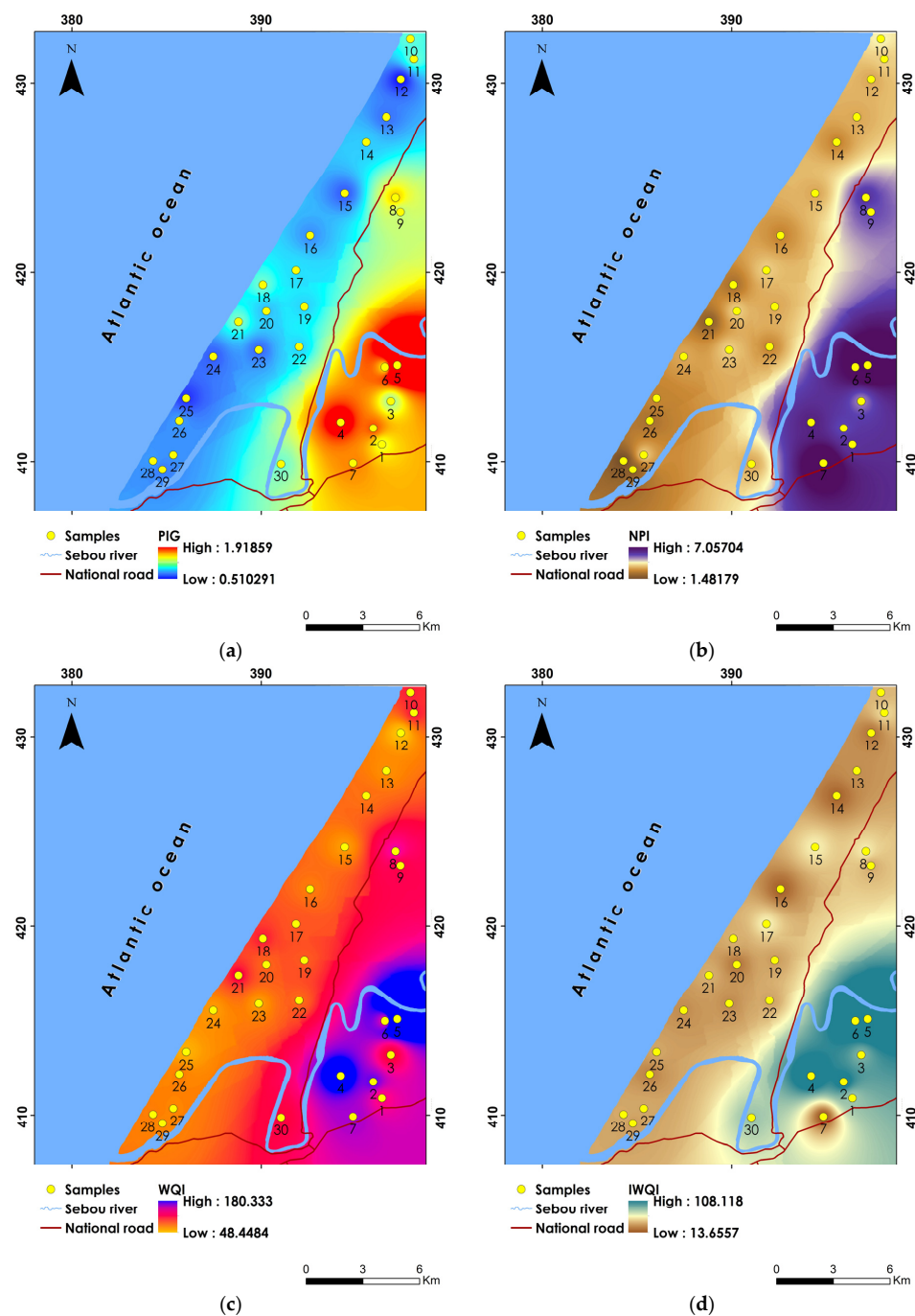


Figure 8. Spatial distribution maps of the (a) PIG, (b) NPI, (c) WQI, and (d) IWQI.

### 3.8. Nitrate Pollution Index (NPI)

The NPI serves as a valuable index for assessing groundwater pollution resulting from heightened nitrate concentrations [38]. The analysis of the NPI values (Table 10) reveals that samples collected from locations P21, P28, and P29 exhibit values of 1.79, 1.48, and 1.79, respectively, categorizing them under “Moderate pollution” (ranging from 1 to 2), comprising 10% of the total samples. Notably, 40% of the sample locations fall within the classification of “Significant pollution” (ranging from 2 to 3), while the remaining 50% are categorized as experiencing “Very significant” pollution (exceeding 3). Across the study area, the NPI ranges from 1.48 to 7.06, with an average value of 3.29, indicative of a pronounced and concerning level of nitrate pollution prevailing in the region.

The spatial distribution depicted in Figure 8b illustrates the NPI values, revealing that the southeastern region of the area exhibits significantly high levels of nitrate pollution. This observation underscores the global significance of nitrate contamination in the Mnasra region, characterized by sandy soils known for their high permeability and infiltration rates, which facilitate the accumulation of nitrate [69]. In agricultural regions with sandy soils, the capacity to retain such elements is generally low, thereby allowing nitrate ions to easily percolate into groundwater through rainfall or irrigation. However, inadequate irrigation management can exacerbate water misuse and lead to adverse environmental impacts, including nitrate pollution and eutrophication [70,71]. Numerous studies conducted in the Mnasra region consistently report elevated levels of nitrates [13,15,16].

Agricultural activities have been identified as significant contributors to groundwater pollution in various studies [72,73]. Factors such as limited soil coverage, excessive fertilization, runoff and infiltration of surplus fertilizers, drainage systems, and the utilization of organic fertilizers from animal husbandry and wastewater reuse all contribute to nitrate pollution [74].

### 3.9. Water Quality Index (WQI)

The WQI was employed to assess the suitability of groundwater for drinking purposes in accordance with World Health Organization standards. The computed WQI values are presented in Table 10, revealing a range from 48.42 to 180.46 across the 30 samples, with an average of 75.39. The analysis indicates that the majority of samples fall within the “good” water quality class for drinking, accounting for 83.33% of the total. Sample P12 exhibited excellent water quality with a WQI below 50, specifically scoring 48.42, thus classified as “excellent” for consumption. Conversely, samples P2, P4, P5, and P7 are deemed unsuitable for drinking purposes, classified as “poor” water quality with WQI values ranging from 100 to 200, collectively representing 13.33%. The spatial distribution of WQI, as depicted in Figure 8c, highlights that groundwater samples collected from the southeast region of the Mnasra area are unfit for drinking purposes.

### 3.10. Irrigation Water Quality Index (IWQI)

It is essential to assess the suitability of groundwater for irrigation purposes as it constitutes the primary water source for agricultural activities [75]. In this study, several parameters including EC, SAR, RSC, Na%, MAR, IP, RSBC, KI, and PS are considered to determine the suitability of groundwater for irrigation. The classification of groundwater samples based on these parameters is presented in Table 11. Additionally, a graphical representation illustrating the suitability of water samples for irrigation purposes was constructed using the US Salinity and Wilcox classification systems.

**Table 11.** The IWQ parameters for groundwater samples.

IWQ Parameters	Range	Class	Number of Samples
EC	<250	Excellent	-
	250–750	Good	23
	750–2250	Doubtful	5
	>2500	Unsuitable	2
SAR	<10	Excellent	30
	10–18	Good	-
	19–26	Doubtful	-
	>26	Unsuitable	-
RSC	<1.25	Good	30
	1.25–2.5	Doubtful	-
	>2.5	Unsuitable	-
Na %	<20	Excellent	25
	20–40	Good	5
	40–60	Permissible	-
	60–80	Doubtful	-
	>80	Unsuitable	-
MAR	<50%	Suitable	21
	>50%	Unsuitable	9
IP	>75%	Good	-
	25–75%	Suitable	5
	<25%	Unsuitable	25
RSBC	<0	Satisfactory	30
	0		-
	0–2.5		-
	2.5–5	Marginal	-
	5–10		-
	>10		-
KI	<1	Suitable	30
	>1	Unsuitable	-
PS	<3	Excellent	2
	3–5	Good	10
	>5	Unsuitable	18

The EC is a key parameter for assessing the salinity hazard and determining the suitability of irrigation water, as it directly influences plant growth and crop production [19]. Based on Wilcox’s classification system, irrigation water salinity is categorized into five classes according to EC values (Table 11). The analysis of groundwater samples revealed that the majority (76%) fell within the “good” class, covering most of the studied area, while five samples were classified as “doubtful” and only two samples as “unsuitable”.

The SAR provides valuable insights into the relative activity of sodium cations in ion exchange reactions with soil properties [76]. Elevated SAR values can adversely affect soil properties such as permeability and soil particle dispersion [77]. The SAR values in our study ranged from 0.09 to 1.74 meq/L, with an average of 0.47 meq/L, with higher values observed in the northwest and southeast regions (Figure 9a).

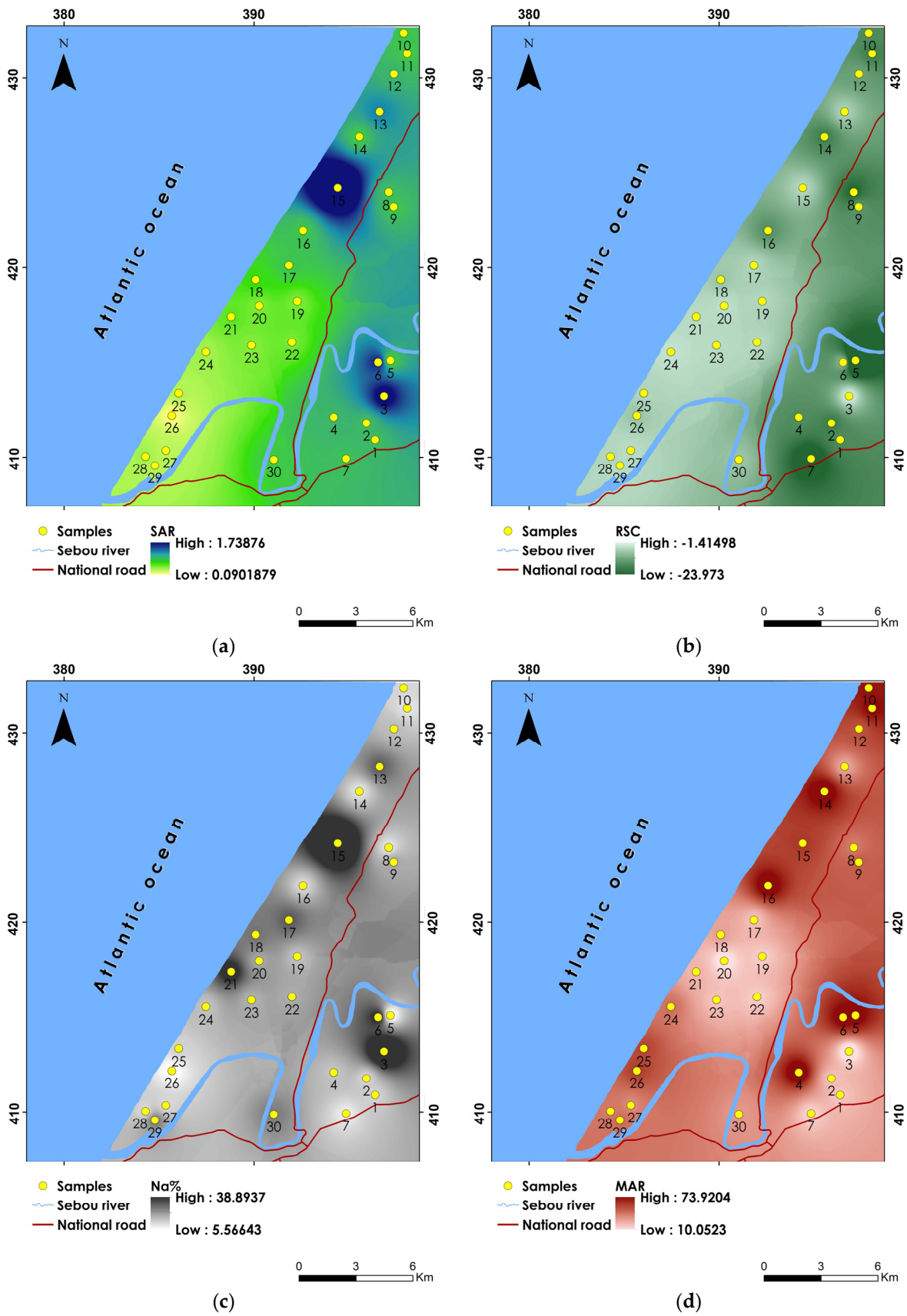


Figure 9. Spatial variation of the IWQ parameters (a) SAR, (b) RSC, (c) Na% and (d) MAR.

All samples were classified as “good” according to Richards [78] classification system (Table 11). Utilizing the USSL diagram, which plots EC against SAR values (Figure 10), we categorized the irrigation water quality. Approximately 76.66% of groundwater samples fell into the C2-S1 category, indicating low to medium salinity and low sodium content. Additionally, 16.66% of samples fell into the C3-S1 category, representing medium salinity and low sodium content in surface waters. Two samples, P4 and P5, were categorized as C4-S1 and C5-S1, respectively, indicating medium salinity groundwater within the study area (<2250  $\mu\text{S}/\text{cm}$ ).

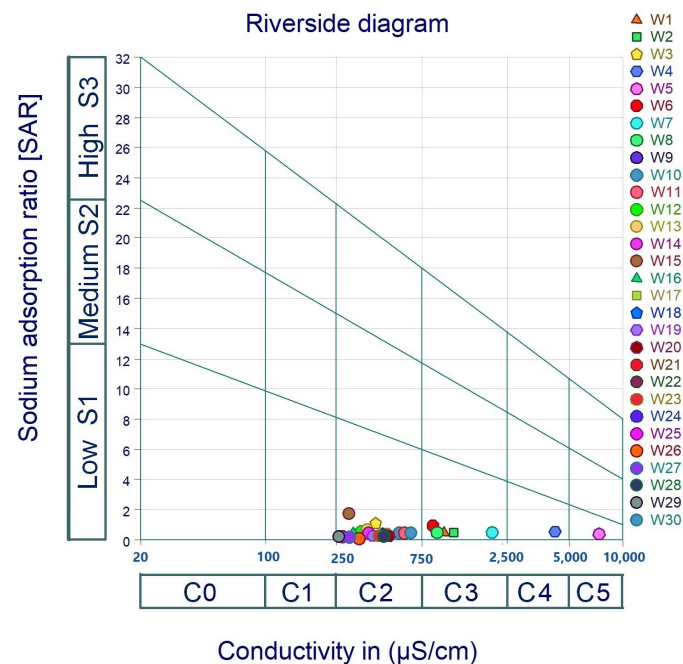


Figure 10. USSL diagram.

The elevated sodium content in groundwater poses a significant threat to soil structure, soil permeability, and crop productivity. The Na% values from collected samples were categorized into five classes following the recommended [47] guidelines. The analysis of the Wilcox graph scatter plot (Figure 11) indicates that the majority (76.66%) of groundwater samples are classified as excellent to good, while 16.66% fall within the good to permissible range. However, 6.66% of samples (P4 and P5) are categorized as doubtful and unsuitable for irrigation purposes. Further classification based on Na% is presented in Table 11, revealing that 83.33% of samples are rated as “excellent”, and 16.66% as “good”. The Na% values range from 5.54% to 38.92%, with an average of 15.11%. Notably, the highest Na% values are observed in the northwest, western, and southeast regions of the study area (Figure 9c).

The RSC serves as a crucial parameter in assessing groundwater suitability for irrigation, focusing on the potential hazards posed by carbonate and bicarbonate ions to calcium and magnesium levels [77,79]. A negative RSC value indicates a minimal risk of sodium accumulation, signifying a balance between calcium and magnesium levels, whereas positive values signify sodium buildup due to bicarbonate and carbonate ions [30]. In our study area, all groundwater samples exhibited negative RSC values, indicating low risk and categorizing them as “good” for irrigation (Table 11).

The MAR categorizes water suitability into two classes:  $\text{MAR} > 50\%$  denotes suitability for agricultural purposes, while  $\text{MAR} < 50\%$  indicates unsuitability. Our findings reveal that approximately 70% of samples are deemed suitable for irrigation, as indicated in (Table 11). The spatial analysis of MAR values indicates that unsuitable water ( $\text{MAR} < 50\%$ ) is predominantly located in the northwest and southeast regions of the study area (Figure 9d).

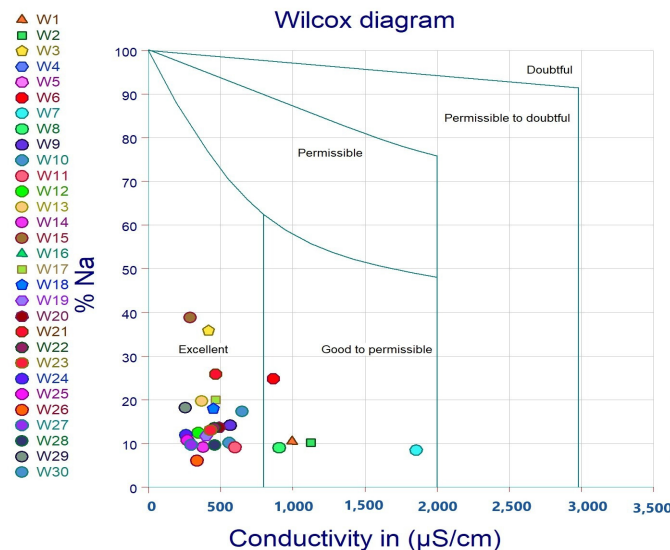


Figure 11. Wilcox diagram for irrigation water quality.

The PI is a crucial parameter in assessing irrigation water, directly influenced by sodium, calcium, magnesium, and bicarbonate concentrations, which significantly affect soil permeability [80]. Following the classification presented in [81], PI is categorized into three classes: class I (>75%) is suitable, class II (25–75%) is good, and class III (<25%) is unsuitable for irrigation. Our study reports PI values ranging from 8.94% to 52.96%, with an average value of 21.44%. Table 11 illustrates that 16.33% and 83.33% of samples fall under suitable to unsuitable categories for irrigation, respectively. Higher PI values are observed in the northwest, southeast, and south regions of the study area (Figure 12a).

The RSBC serves as an indicator of alkalinity risk [82]. In our study, all groundwater samples exhibited negative RSBC values, indicating their suitability for irrigation use (Table 11).

Kelly (1957) introduced the KR, where a KR value < 1 indicates suitable irrigation water, while values > 1 are deemed unsuitable. Our findings show KR values ranging from 0.03% to 0.63%, with an average value of 0.16%. Consequently, all 30 water samples in our study area were classified as unsuitable for irrigation (Table 11).

The PS for assessing groundwater salinity was introduced by the work presented in [81], calculated as the concentration of  $Cl^-$  plus half the concentration of  $SO_4^{2-}$ . In our analysis, the potential salinity ranged from 2.34 meq/L to 22.20 meq/L, with an average of 7.76 meq/L (Table 11). This categorizes 60% of samples as unsuitable, 33.33% as good, and samples P15 and P16 as excellent. The elevated values observed in the southeast region could be attributed to the increased concentration in chloride, potentially influenced by seawater intrusion (Figure 12d).

The IWQI considers nine indices (Table 11), with values ranging from 13.63 to 108.18 and an average of 37.34 for all samples (Table 10). Comparing with water quality classifications, 80% of samples were deemed “excellent”, 16.66% “good” (samples P2, P3, P4, P6, P30), and sample P5 classified as “poor”. Spatial analysis of the IWQI indicates low-quality water predominating in the eastern and southern sections, with the southern portion particularly affected by agricultural activities such as fertilizer overuse, irrigation, and wastewater (Figure 8d). Sample P5 exhibits high contamination and salinization, likely attributed to geological sources or rock formations.

Geologically, the presence of permeable layers, such as sands and sandstones, facilitates contaminant movement, while impermeable layers offer some degree of protection. Hydrological factors, including groundwater flow direction and velocity, significantly influence the spread and transport of pollutants within aquifers.

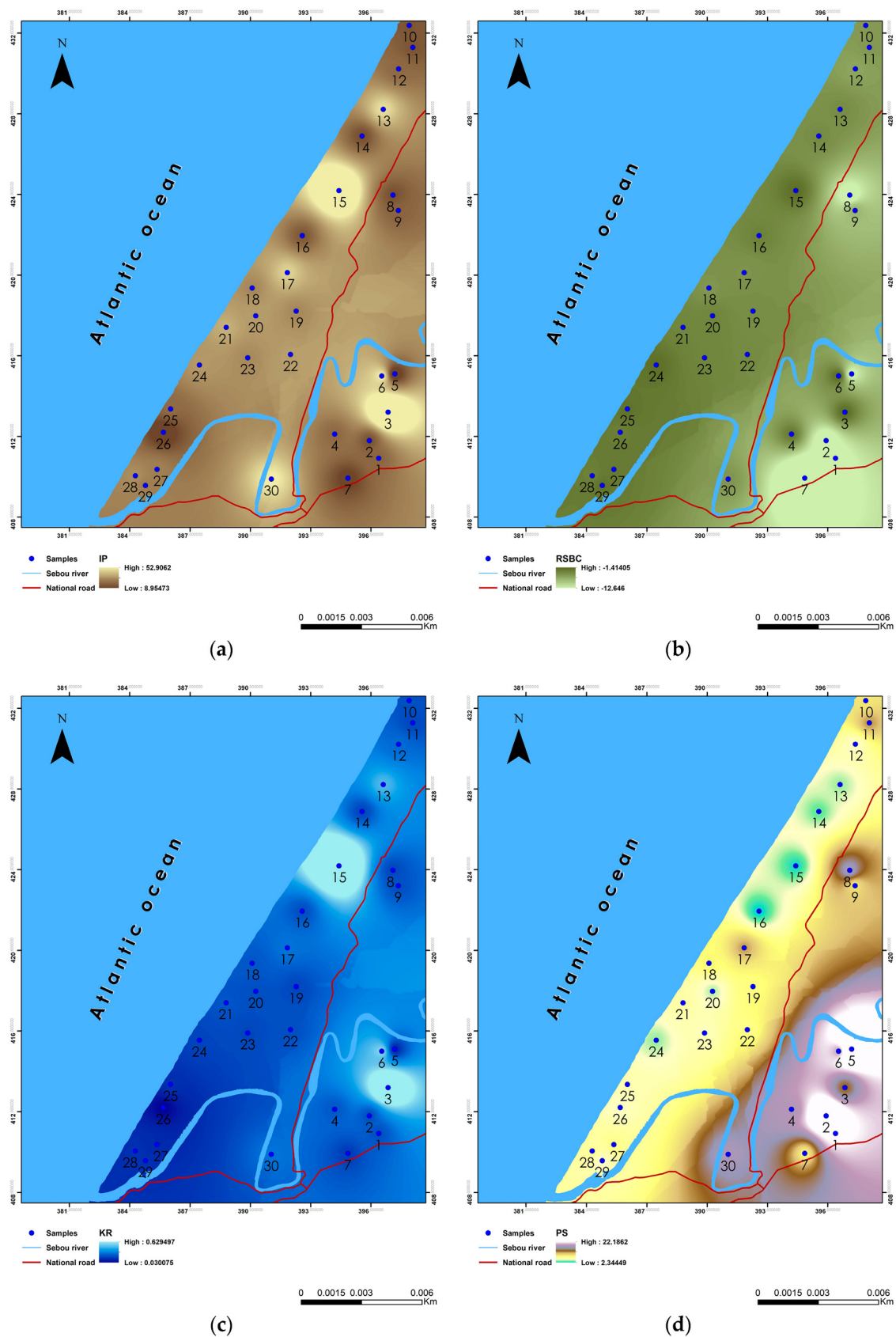


Figure 12. Spatial variation of the IWQ parameters (a) IP, (b) RSBC, (c) KI and (d) PS.

#### 4. Conclusions

Groundwater serves as a vital resource for meeting the water demands in Morocco, yet it confronts significant challenges. The confluence of escalating water needs and diminished precipitation resulting from climate change has placed a substantial strain on groundwater reservoirs across the nation. The quality of groundwater is a pivotal factor in assessing human well-being and development. This study endeavors to evaluate and delineate the origins of groundwater contamination associated with both natural and anthropogenic sources in an agricultural region of the Gharb Plain, employing hydrochemical methodologies, index techniques (such as PIG, NPI, WQI, and IWQI), multivariate statistical analyses, and GIS approaches. The originality of this research lies in its comprehensive approach, integrating diverse methodologies to identify and understand the sources of groundwater pollution. The investigation encompasses thirty groundwater samples collected from various locations to assess their characteristics, focusing on 23 physicochemical parameters.

The study findings reveal that  $\text{Ca}^{2+}$  and  $\text{Cl}^{-}$  are the predominant cation and anion, respectively, within the study area. The analysis using the Piper diagram indicates a prevailing water type of  $\text{Ca}^{2+}\text{-Cl}^{-}$ , while the Gibbs diagram highlights that water–rock interactions significantly influence groundwater chemistry, with all samples falling within the field of rock dominance. The PIG values range from 0.51 to 1.92, with the majority (86.66%) falling under the category of “Insignificant pollution”, indicating suitability for rural consumption. However, some wells exhibit “low pollution”, with the highest PIG value of 1.92, attributed to anthropogenic activities, marking it as “moderate pollution”. The NPI ranges from 1.48 to 7.06, signifying concerning levels of nitrate contamination linked to anthropogenic activities such as fertilizers and sewage intrusion. The WQI analysis reveals that 83.33% of samples are of “good” quality for drinking, with one sample classified as “excellent”, while four samples are deemed unsuitable (“poor”). Regarding irrigation suitability, most parameters (EC, SAR, RSC, Na%, MAR, RSBC) indicate appropriateness, except for IP, KR, and PS, which deem samples unsuitable. The IWQI ranges from 13.63 to 108.18, with 80% classified as “excellent” and 16.66% as “good”, except for one sample categorized as “poor”. Spatial analysis identifies the eastern and southern regions as the most contaminated due to intensive pesticide use and agricultural activities, compounded by the unregulated discharge of polluted water from the Sebou River.

This study provides a comprehensive overview of the current groundwater status in the research area, offering valuable insights for policymakers and relevant authorities. In addressing groundwater pollution challenges, particularly in Morocco’s Gharb region, the adoption of sustainable agricultural practices, efficient land utilization, and effective water management strategies is imperative. Encouraging the implementation of methods like crop rotation, precision irrigation, and optimized water usage can significantly mitigate the ingress of pollutants into groundwater reservoirs. Prioritizing fertilizer management is crucial to combat excessive nitrate infiltration into groundwater sources. Implementing measures such as regulating fertilizer application timing and quantities, along with utilizing organic residues as alternative fertilizers, can help to maintain nutrient equilibrium and reduce leaching.

**Author Contributions:** Conceptualization, H.S. and A.Z.; methodology, H.S., H.E.A. and A.Z.; software, H.S. and H.E.A.; Resources, H.S., H.E.A., H.Y., M.O.L. and A.G.; validation, H.S., L.M., A.Z. and H.D.; formal analysis, H.S., L.M., A.Z., R.M., H.E.A. and H.D.; writing—original draft preparation, H.S., A.Z., H.E.A., M.O.L. and H.D.; writing—review and editing, H.S., L.M., A.Z., R.M., H.E.A., A.G., H.Y., M.O.L. and H.D.; visualization, H.S., H.E.A. and A.Z.; supervision, H.D. and L.M.; funding acquisition, R.M. All authors have read and agreed to the published version of the manuscript.

**Funding:** This research received no external funding.

**Data Availability Statement:** The authors strongly encourage interested researchers to contact us, as we are more than willing to share the data upon request.

**Acknowledgments:** The authors would like to thank all those who collaborated in this work on the field sampling, laboratory analysis, and writing manuscript teams from laboratory of Process Engineering and Environment, National Institute of Agricultural Research (INRA), International Center for Agricultural Research in the Dry Areas (ICARDA) in Morocco. The authors would like to thank the “MCGP” and “Climber” projects for their financial support.

**Conflicts of Interest:** The authors declare no conflicts of interest.

## References

- Zhang, Q.; Li, Y.; Kong, Q.; Huang, H. Coupling Coordination Analysis and Key Factors between Urbanization and Water Resources in Ecologically Fragile Areas: A Case Study of the Yellow River Basin, China. *Environ. Sci. Pollut. Res.* **2024**, *31*, 10818–10837. [[CrossRef](#)] [[PubMed](#)]
- Saima, A.; Yahya, B.; Tabasum, Y.; Maqsooda, A.; Sinan, N. Water Quality Assessment in Relation to Fish Assemblage Using Multivariate Analysis in Manasbal Lake, Kashmir. *Water Sci.* **2024**, *38*, 92–108. [[CrossRef](#)]
- Al-Qawati, M.; El-Qaysy, M.; Darwish, N.; Sibbari, M.; Hamdaoui, F.; Kherrati, I.; El Kharrim, K.; Belghyti, D. Hydrogeochemical Study of Groundwater Quality in the West of Sidi Allal Tazi, Gharb Area, Morocco. *J. Mater. Environ. Sci.* **2018**, *9*, 293–304. [[CrossRef](#)]
- Guyo, R.H.; Wang, K.; Saito, M.; Onodera, S.; Shimizu, Y.; Moroizumi, T. Spatiotemporal Shallow and Deep Groundwater Dynamics in a Forested Mountain Catchment with Diverse Slope Gradients, Western Japan. *Groundw. Sustain. Dev.* **2024**, *25*, 101150. [[CrossRef](#)]
- Sharma, K.; Rajan, S.; Nayak, S.K. Chapter 1—Water Pollution: Primary Sources and Associated Human Health Hazards with Special Emphasis on Rural Areas. In *Water Resources Management for Rural Development*; Elsevier: Amsterdam, The Netherlands, 2024; pp. 3–14.
- Bouita, M.; El Mahdi, Y.; Sbai, H.; Bouita, I.; El Bakouri, A.; Ibrahimi, E.M.; Chakir, E.M. Assessment of Nitrogen Pollution of Groundwater in the Maamora Gharb Aquifer, Morocco. *Egypt. J. Aquat. Biol. Fish.* **2021**, *25*, 739–758. [[CrossRef](#)]
- Ez-zaouy, Y.; Bouchaou, L.; Saad, A.; Hssaisoune, M.; Brouziyne, Y.; Dhiba, D.; Chehbouni, A. Morocco’s Coastal Aquifers: Recent Observations, Evolution and Perspectives towards Sustainability. *Environ. Pollut.* **2022**, *293*, 118498. [[CrossRef](#)] [[PubMed](#)]
- Hssaisoune, M.; Bouchaou, L.; Sifeddine, A.; Bouimetarhan, I.; Chehbouni, A. Moroccan Groundwater Resources and Evolution with Global Climate Changes. *Geosciences* **2020**, *10*, 81. [[CrossRef](#)]
- Sehlaoui, H.; Hassikou, R.; Moussadek, R.; Zouahri, A.; Douaik, A.; Iiach, H.; Ghanimi, A.; Dakak, H. Evaluation of Water Quality for Agricultural Suitability in the Benslimane Region, Morocco. *Environ. Monit. Assess.* **2020**, *192*, 587. [[CrossRef](#)] [[PubMed](#)]
- Aabad, M.; Bouaziz, A.; Falisse, A.; Martin, J.F. Improving Yield and Water Use Efficiency of Sugarcane under Drip. *Rev. Marocaine Des Sci. Agron. Et Vétérinaires* **2016**, *5*, 32–40.
- Hammoumi, N.E.; Sinan, M.; Lekhlif, B.; Lakhdar, M. Use of Multivariate Statistical and Geographic Information System (GIS)-Based Approach to Evaluate Ground Water Quality in the Irrigated Plain of Tadla (Morocco). *Int. J. Water Resour. Environ. Eng.* **2013**, *5*, 77–93.
- Nezha, E.M.; Mohamed, E.W.; Rajae, A.; Ridouane, S.; Sanae, B. Evaluation of Vulnerability of the Underground Aquifer of the Gharb Plain with the Help of Gis and Drastic Method (Nw of Morocco). *Eur. Sci. J. ESJ* **2016**, *12*, 387. [[CrossRef](#)]
- Omrana, S.; El Khodrani, N.; Zouahri, A.; Douaik, A.; Iaaich, H.; Lahmar, M.; Hajjaji, E. Physico-Chemical Characterization of Water and Soil of the M’nasra Region in the Gharb Plain (Northwest Morocco). *Moroc. J. Chem.* **2019**, *7*, 482–492.
- Maftouh, I.; Moussaif, A.; Elmzibri, M.; Elabbadi, N.; Mesfioui, A. Assessment of the Main Active Molecules among the Most Used Pesticides in the Gharb Region in Morocco. *Int. J. Agric. Innov. Res.* **2017**, *6*, 359–362.
- Aziane, N.; Khaddari, A.; IbenTouhami, M.; Zouahri, A.; Nassali, H.; Elyoubi, M.S. Evaluation of Groundwater Suitability for Irrigation in the Coastal Aquifer of Mnasra (Gharb, Morocco). *Mediterr. J. Chem.* **2020**, *10*, 197–212. [[CrossRef](#)]
- Marouane, B.; Dahchour, A.; Dousset, S.; El Hajjaji, S. Monitoring of Nitrate and Pesticide Pollution in Mnasra, Morocco Soil and Groundwater. *Water Environ. Res.* **2015**, *87*, 567–575. [[CrossRef](#)] [[PubMed](#)]
- Rawat, M.; Sen, R.; Onyekwelu, I.; Wiederstein, T.; Sharda, V. Modeling of Groundwater Nitrate Contamination Due to Agricultural Activities—A Systematic Review. *Water* **2022**, *14*, 4008. [[CrossRef](#)]
- Wang, H.; Gao, J.; Li, X.; Zhang, S.; Wang, H. Nitrate Accumulation and Leaching in Surface and Ground Water Based on Simulated Rainfall Experiments. *PLoS ONE* **2015**, *10*, e0136274. [[CrossRef](#)] [[PubMed](#)]
- Hosseini, M.; Hassanzadeh, R. Groundwater Quality Assessment for Domestic and Agricultural Purposes Using GIS, Hydrochemical Facies and Water Quality Indices: Case Study of Rafsanjan Plain, Kerman Province, Iran. *Appl. Water Sci.* **2023**, *13*, 84. [[CrossRef](#)]
- Sunitha, V.; Reddy, B.M. Geochemical Characterization, Deciphering Groundwater Quality Using Pollution Index of Groundwater (PIG), Water Quality Index (WQI) and Geographical Information System (GIS) in Hard Rock Aquifer, South India. *Appl. Water Sci.* **2022**, *12*, 41. [[CrossRef](#)]
- Azhari, H.E.; Cherif, E.K.; Sarti, O.; Azzirgue, E.M.; Dakak, H.; Yachou, H.; Esteves Da Silva, J.C.G.; Salmoun, F. Assessment of Surface Water Quality Using the Water Quality Index (IWQ), Multivariate Statistical Analysis (MSA) and Geographic Information System (GIS) in Oued Laou Mediterranean Watershed, Morocco. *Water* **2022**, *15*, 130. [[CrossRef](#)]

22. El Mountassir, O.; Bahir, M.; Chehbouni, A.; Dhiba, D.; El Jiar, H. Assessment of Groundwater Quality and the Main Controls on Its Hydrochemistry in a Changing Climate in Morocco (Essaouira Basin). *Sustainability* **2022**, *14*, 8012. [[CrossRef](#)]
23. Vaiphei, S.P.; Kurakalva, R.M.; Sahadevan, D.K. Water Quality Index and GIS-Based Technique for Assessment of Groundwater Quality in Wanaparthy Watershed, Telangana, India. *Environ. Sci. Pollut. Res.* **2020**, *27*, 45041–45062. [[CrossRef](#)] [[PubMed](#)]
24. Mallick, J.; Kumar, A.; Almesfer, M.K.; Alsubih, M.; Singh, C.K.; Ahmed, M.; Khan, R.A. An Index-Based Approach to Assess Groundwater Quality for Drinking and Irrigation in Asir Region of Saudi Arabia. *Arab. J. Geosci.* **2021**, *14*, 157. [[CrossRef](#)]
25. Horton, R.K.; Horton, R.K. An Index Number System for Rating Water Quality. *J. Water Poll. Cont. Fed.* **1965**, *37*, 300–306.
26. Radouane, E.M.; Chahlaoui, A.; Maliki, A.; Boudellah, A. Assessment and Modeling of Groundwater Quality by Using Water Quality Index (WQI) and GIS Technique in Meknes Aquifer (Morocco). *Geol. Ecol. Landsc.* **2023**, *7*, 126–138. [[CrossRef](#)]
27. Masoud, M.; El Osta, M.; Alqarawy, A.; Elsayed, S.; Gad, M. Evaluation of Groundwater Quality for Agricultural under Different Conditions Using Water Quality Indices, Partial Least Squares Regression Models, and GIS Approaches. *Appl. Water Sci.* **2022**, *12*, 244. [[CrossRef](#)]
28. Elemile, O.O.; Ibitogbe, E.M.; Okikiola, B.T.; Ejigboye, P.O. Groundwater Quality Using Indices for Domestic and Irrigation Purposes in Akure, Nigeria. *Results Eng.* **2022**, *13*, 100347. [[CrossRef](#)]
29. Batarseh, M.; Imreizeeq, E.; Tilev, S.; Alaween, M.A.; Suleiman, W.; Remeithi, A.M.A.; Tamimi, M.K.A.; Alawneh, M.A. Assessment of Groundwater Quality for Irrigation in the Arid Regions Using Irrigation Water Quality Index (IWQI) and GIS-Zoning Maps: Case Study from Abu Dhabi Emirate, UAE. *Groundw. Sustain. Dev.* **2021**, *14*, 100611. [[CrossRef](#)]
30. Jesuraja, K.; Selvam, S.; Murugan, R. GIS-Based Assessment of Groundwater Quality Index (DWQI and AWQI) in Tiruchendur Coastal City, Southern Tamil Nadu, India. *Environ. Earth Sci* **2021**, *80*, 243. [[CrossRef](#)]
31. Jeddi, F.; Berradi, M.; Harfi, A.E.; Aboussaloua, E.H. Characterization of Physicochemical Parameters of the Pollution of Wade Beht Waters in Gharb-Morocco Region. *Appl. J. Environ. Eng. Sci.* **2017**, *3*, 201–208.
32. Kaiser, H.F. The Varimax Criterion for Analytic Rotation in Factor Analysis. *Psychometrika* **1958**, *23*, 187–200. [[CrossRef](#)]
33. Rodier, J. *L'analyse de L'eau, Eaux Naturelles, Eaux Résiduaires, Eau de Mer*, 7th ed.; Dunod: Paris, France, 1985.
34. Subba Rao, N. PIG: A Numerical Index for Dissemination of Groundwater Contamination Zones. *Hydrol. Process.* **2012**, *26*, 3344–3350. [[CrossRef](#)]
35. Al-Aizari, H.S.; Aslaou, F.; Al-Aizari, A.R.; Al-Odayni, A.-B.; Al-Aizari, A.-J.M. Evaluation of Groundwater Quality and Contamination Using the Groundwater Pollution Index (GPI), Nitrate Pollution Index (NPI), and GIS. *Water* **2023**, *15*, 3701. [[CrossRef](#)]
36. Subba Rao, N. Groundwater Quality from a Part of Prakasam District, Andhra Pradesh, India. *Appl. Water Sci.* **2018**, *8*, 30. [[CrossRef](#)]
37. WHO World Health Organization. *Guidelines for Drinking-Water Quality: Fourth Edition Incorporating First Addendum*; World Health Organization: Geneva, Switzerland, 2017; ISBN 978-92-4-154995-0.
38. Panneerselvam, B.; Karuppannan, S.; Muniraj, K. Evaluation of Drinking and Irrigation Suitability of Groundwater with Special Emphasizing the Health Risk Posed by Nitrate Contamination Using Nitrate Pollution Index (NPI) and Human Health Risk Assessment (HHRA). *Hum. Ecol. Risk Assess. Int. J.* **2021**, *27*, 1324–1348. [[CrossRef](#)]
39. Kachroud, M.; Trolard, F.; Kefi, M.; Jebari, S.; Bourrié, G. Water Quality Indices: Challenges and Application Limits in the Literature. *Water* **2019**, *11*, 361. [[CrossRef](#)]
40. Kadri, A.; Baouia, K.; Kateb, S.; Al-Ansari, N.; Kouadri, S.; Najm, H.M.; Mashaan, N.S.; Eldirderi, M.M.A.; Khedher, K.M. Assessment of Groundwater Suitability for Agricultural Purposes: A Case Study of South Oued Righ Region, Algeria. *Sustainability* **2022**, *14*, 8858. [[CrossRef](#)]
41. Beyene, G.; Aberra, D.; Fufa, F. Evaluation of the Suitability of Groundwater for Drinking and Irrigation Purposes in Jimma Zone of Oromia, Ethiopia. *Groundw. Sustain. Dev.* **2019**, *9*, 100216. [[CrossRef](#)]
42. Bian, J.; Nie, S.; Wang, R.; Wan, H.; Liu, C. Hydrochemical Characteristics and Quality Assessment of Groundwater for Irrigation Use in Central and Eastern Songnen Plain, Northeast China. *Environ. Monit. Assess.* **2018**, *190*, 382. [[CrossRef](#)]
43. Karunanidhi, D.; Aravinthasamy, P.; Kumar, D.; Subramani, T.; Roy, P.D. Sobol Sensitivity Approach for the Appraisal of Geomedical Health Risks Associated with Oral Intake and Dermal Pathways of Groundwater Fluoride in a Semi-Arid Region of South India. *Ecotoxicol. Environ. Saf.* **2020**, *194*, 110438. [[CrossRef](#)]
44. Raju, N.J. Hydrogeochemical Parameters for Assessment of Groundwater Quality in the Upper Gunjanaeru River Basin, Cuddapah District, Andhra Pradesh, South India. *Environ. Geol.* **2007**, *52*, 1067–1074. [[CrossRef](#)]
45. Chidambaram, S.; Prasanna, M.; Venkatramanan, S.; Nepolian, M.; Pradeep, K. Groundwater Quality Assessment for Irrigation by Adopting New Suitability Plot and Spatial Analysis Based on Fuzzy Logic Technique. *Environ. Res.* **2022**, *204*, 111729.
46. Guo, H.; Li, M.; Wang, L.; Wang, Y.; Zang, X.; Zhao, X.; Wang, H.; Zhu, J. Evaluation of Groundwater Suitability for Irrigation and Drinking Purposes in an Agricultural Region of the North China Plain. *Water* **2021**, *13*, 3426. [[CrossRef](#)]
47. Wilcox, L. *Classification and Use of Irrigation Water*, 4th ed.; USDA, Circular: Washington, DC, USA, 1955; p. 969.
48. USSL Salinity Laboratory. *Diagnosis and Improvement of Saline and Alkaline Soils*; US Department of Agriculture Handbook; No. 60; US Department of Agriculture: Washington, DC, USA, 1954.
49. Zouahri, A.; Dakak, H.; Douaik, A.; El Khadir, M.; Moussadek, R. Evaluation of Groundwater Suitability for Irrigation in the Skhirat Region, Northwest of Morocco. *Environ. Monit. Assess.* **2015**, *187*, 4184. [[CrossRef](#)]

50. El Khodrani, N.; Zouahri, A.; Douaik, A.; Omrania, S.; Iaaich, H.; Yahyaoui, A. Fekhaoui Evaluation the Impact of Intensive Agriculture on Physic- Chemical Properties of Soil and Groundwater in the Rural Commune Sfaaa. *J. Mater. Environ. Sci.* **2017**, *8*, 2339–2346.
51. Mouna, M.; Redouane, C.-A.; Lhoussaine, B.; Yassine, A.B.; Abdelaziz, H.; Reichert, B. Evolution of Groundwater Quality in Intensive Agricultural Zone: Case of Chtouka-Massa Aquifer, Morocco. *Arab. J. Geosci.* **2016**, *9*, 566. [[CrossRef](#)]
52. Moukhliis, M.; Taleb, A.; Khattabi Rifi, S.; El fathi, B.; El bilali, A.; Souabi, S. Assessment of Groundwater Quality in Berrechid Aquifer, Morocco. *Moroc. J. Chem.* **2021**, *9*, 800–812.
53. Nshimiyimana, F.X.; Blidi, S.E.; Abidi, A.E.; Faciu, M.E.; Udahemuka, J.C.; Lazar, G.; Soulaymani, A.; Fekhaoui, M. Groundwater Quality from the El Aarjate Zone (Morocco). *J. Mater. Environ. Sci.* **2016**, *7*, 2760–2770.
54. Lahmar, M.; Khodrani, N.E.; Omrania, S.; Dakak, H.; Douaik, A.; Iaaich, H.; El, M.; Mekkaoui, M.; Zouahri, A. Assesment of the Physico-Chemical Quality of Groundwater in the Sidi Yahya Region, Gharb, Morocco. *Moroc. J. Chem.* **2019**, *7*, 424–430.
55. Nouzha, B.; Kacem, S.A.; Ferdaouss, L.; Aberrahim, L.; Mohammed, B. Evaluation De L'impact De La Pollution Agricole Sur La Qualite Des Eaux Souterraines De La Nappe Du Gharb. *Eur. Sci. J. ESJ* **2016**, *12*, 509. [[CrossRef](#)]
56. Sefiani, S.; El Mandour, A.; Laftouhi, N.; Khalil, N.; Chehbouni, A.; Jarlan, L.; Hanich, L.; Khabba, S.; Kamal, S.; Markhi, A.; et al. Evaluation of Groundwater Quality and Agricultural Use Under a Semi-arid Environment: Case of Agafay, Western Haouz, Morocco. *Irrig. Drain.* **2019**, *68*, 778–796. [[CrossRef](#)]
57. Das, S.; Nag, S.K. Application of Multivariate Statistical Analysis Concepts for Assessment of Hydrogeochemistry of Groundwater—A Study in Suri I and II Blocks of Birbhum District, West Bengal, India. *Appl. Water Sci.* **2017**, *7*, 873–888. [[CrossRef](#)]
58. Wu, J.; Li, P.; Qian, H.; Duan, Z.; Zhang, X. Using Correlation and Multivariate Statistical Analysis to Identify Hydrogeochemical Processes Affecting the Major Ion Chemistry of Waters: A Case Study in Laoheba Phosphorite Mine in Sichuan, China. *Arab. J. Geosci.* **2014**, *7*, 3973–3982. [[CrossRef](#)]
59. Howladar, M.F.; Deb, P.K.; Muzemder, A.T.M.S.H.; Ahmed, M. Evaluation of Water Resources around Barapukuria Coal Mine Industrial Area, Dinajpur, Bangladesh. *Appl. Water Sci.* **2014**, *4*, 203–222. [[CrossRef](#)]
60. Bahir, M.; Ouhamdouch, S.; Ouazar, D.; Moçayd, N.E. Climate Change Effect on Groundwater Characteristics within Semi-Arid Zones from Western Morocco. *Groundw. Sustain. Dev.* **2020**, *11*, 100380. [[CrossRef](#)]
61. Rabeiy, R.E. Assessment and Modeling of Groundwater Quality Using WQI and GIS in Upper Egypt Area. *Environ. Sci. Pollut. Res.* **2018**, *25*, 30808–30817. [[CrossRef](#)]
62. Abbas, H.; Abuzaid, A.; Jahin, H.; Kasem, D. Assessing the Quality of Untraditional Water Sources for Irrigation Purposes in Al-Qalubiya Governorate, Egypt. *Egypt. J. Soil Sci.* **2020**, *60*, 157–166. [[CrossRef](#)]
63. Vincy, M.V.; Brilliant, R.; Pradeepkumar, A.P. Hydrochemical Characterization and Quality Assessment of Groundwater for Drinking and Irrigation Purposes: A Case Study of Meenachil River Basin, Western Ghats, Kerala, India. *Environ. Monit. Assess.* **2014**, *187*, 4217. [[CrossRef](#)] [[PubMed](#)]
64. Machiwal, D.; Jha, M.K. Identifying Sources of Groundwater Contamination in a Hard-Rock Aquifer System Using Multivariate Statistical Analyses and GIS-Based Geostatistical Modeling Techniques. *J. Hydrol. Reg. Stud.* **2015**, *4*, 80–110. [[CrossRef](#)]
65. Ward, J.H., Jr. Hierarchical Grouping to Optimize an Objective Function. *J. Am. Stat. Assoc.* **1963**, *58*, 236–244. [[CrossRef](#)]
66. Piper, A.M. A Graphic Procedure in the Geochemical Interpretation of Water-Analyses. *Eos Trans. Am. Geophys. Union* **1944**, *25*, 914–928. [[CrossRef](#)]
67. Gibbs, R.J. Mechanisms Controlling World Water Chemistry. *Science* **1970**, *170*, 1088–1090. [[CrossRef](#)] [[PubMed](#)]
68. Subba Rao, N. Seasonal Variation of Groundwater Quality in a Part of Guntur District, Andhra Pradesh, India. *Environ. Geol.* **2006**, *49*, 413–429. [[CrossRef](#)]
69. Pan, Y.; She, D.; Ding, J.; Abulaiti, A.; Zhao, J.; Wang, Y.; Liu, R.; Wang, F.; Shan, J.; Xia, Y. Coping with Groundwater Pollution in High-Nitrate Leaching Areas: The Efficacy of Denitrification. *Environ. Res.* **2024**, *250*, 118484. [[CrossRef](#)] [[PubMed](#)]
70. Benkaddour, R.; Merimi, I.; Szumiata, T.; Hammouti, B. Nitrates in the Groundwater of the Triffa Plain Eastern Morocco. *Mater. Today Proc.* **2020**, *27*, 3171–3174. [[CrossRef](#)]
71. El Khodrani, N.; Omrania, S.; Nouayti, A.; Zouahri, A.; Douaik, A.; Iaaich, H.; Lahmar, M.; Fekhaoui, M. Comparative Study of Groundwater Pollution of M'nasra and Sfaaa Zones (Gharb, Morocco) by Nitrates. In *E3S Web of Conferences*; EDP Sciences: Les Ulis, France, 2020; p. 01006.
72. Mohamed, B.; Rachid, M. R'mel Groundwater Quality as Influenced by Agricultural Activities. *Afr. Mediterr. Agric. J.-Al Awamia* **2022**, *137*, 123–138.
73. El Alfy, M.; Faraj, T. Spatial Distribution and Health Risk Assessment for Groundwater Contamination from Intensive Pesticide Use in Arid Areas. *Environ. Geochem. Health* **2017**, *39*, 231–253. [[CrossRef](#)] [[PubMed](#)]
74. Barakat, A.; Mouhtarim, G.; Saji, R.; Touhami, F. Health Risk Assessment of Nitrates in the Groundwater of Beni Amir Irrigated Perimeter, Tadla Plain, Morocco. *Hum. Ecol. Risk Assess. Int. J.* **2020**, *26*, 1864–1878. [[CrossRef](#)]
75. Kumar, P.; Balamurugan, P. Suitability of Ground Water for Irrigation Purpose in Omalur Taluk, Salem, Tamil Nadu, India. *Indian J. Ecol.* **2019**, *46*, 1–6.
76. Adimalla, N. Controlling Factors and Mechanism of Groundwater Quality Variation in Semiarid Region of South India: An Approach of Water Quality Index (WQI) and Health Risk Assessment (HRA). *Environ. Geochem. Health* **2019**, *42*, 1725–1752. [[CrossRef](#)]

77. Selvam, S.; Manimaran, G.; Sivasubramanian, P.; Balasubramanian, N.; Seshunarayana, T. GIS-Based Evaluation of Water Quality Index of Groundwater Resources around Tuticorin Coastal City, South India. *Environ. Earth Sci.* **2014**, *71*, 2847–2867. [[CrossRef](#)]
78. Richards, L.A. Diagnosis and Improvement of Saline and Alkali Soils. *Soil Sci.* **1954**, *78*, 154. [[CrossRef](#)]
79. Bhat, M.A.; Wani, S.A.; Singh, V.K.; Sahoo, J.; Tomar, D.; Sanswal, R.; Ma, B. An Overview of the Assessment of Groundwater Quality for Irrigation. *J. Agric. Sci. Food Res.* **2018**, *9*, 1–9.
80. Rawat, K.S.; Singh, S.K.; Gautam, S.K. Assessment of Groundwater Quality for Irrigation Use: A Peninsular Case Study. *Appl. Water Sci.* **2018**, *8*, 233. [[CrossRef](#)]
81. Doneen, L. Notes on Water Quality in Agriculture. In *Water Science and Engineering Paper 4001*; Department of Water, Science and Engineering, University of California, Davis: Davis, CA, USA, 1964.
82. Mukonazwothe, M.; Munyai, L.F.; Mutoti, M.I. Groundwater Quality Evaluation for Domestic and Irrigation Purposes for the Nwanedi Agricultural Community, Limpopo Province, South Africa. *Heliyon* **2022**, *8*, e09203. [[CrossRef](#)]

**Disclaimer/Publisher’s Note:** The statements, opinions and data contained in all publications are solely those of the individual author(s) and contributor(s) and not of MDPI and/or the editor(s). MDPI and/or the editor(s) disclaim responsibility for any injury to people or property resulting from any ideas, methods, instructions or products referred to in the content.